Inorganic Chemistry

Article

pubs.acs.org/IC

Synthesis and Electrochemical, Photophysical, and Self-Assembly Studies on Water-Soluble pH-Responsive Alkynylplatinum(II) Terpyridine Complexes

Clive Yik-Sham Chung,[†] Steve Po-Yam Li,[‡] Kenneth Kam-Wing Lo,[‡] and Vivian Wing-Wah Yam*[,†]

[†]Institute of Molecular Functional Materials [Areas of Excellence Scheme, University Grants Committee (Hong Kong)] and Department of Chemistry, The University of Hong Kong, Pokfulam Road, Hong Kong, P. R. China

[‡]Department of Biology and Chemistry, City University of Hong Kong, Tat Chee Avenue, Kowloon, Hong Kong, P. R. China

Supporting Information

ABSTRACT: A series of water-soluble pH-responsive alkynylplatinum(II) terpyridine complexes have been synthesized and characterized. The electronic absorption, emission, and electrochemical properties of the complexes have been studied. The self-assembly processes of representative complexes in aqueous media, presumably through Pt···Pt and/or $\pi-\pi$ interactions, have been investigated by concentration- and temperature-dependent UV−vis absorption measurements and dynamic light scattering experiments. Interestingly, some of the complexes have been found to undergo induced self-assembly and disassembly in aqueous media through modulation of the pH value of the solutions, resulting in remarkable UV−vis absorption and emission spectral changes. The emission spectral changes have been rationalized by the change in the hydrophilicity of the complexes, electrostatic repulsion among the complex molecules, and/or the extent of photoinduced electron transfer (PET) quenching upon protonation/deprotonation of the pH-responsive groups on the complexes. By simple modifications of the chemical structures of the complexes, induced self-assembly/disassembly of the complexes can occur at different and/or multiple pH regions, thus allowing the probing of changes at the desired pH region by triplet metal−metal-to-ligand charge-transfer emission of the complexes in the near-infrared (NIR) region. Fixed-cell imaging experiments have further demonstrated the potential of this class of complexes as pH-responsive NIR luminescent probes in vitro, while the NIR emissions of the complexes from live cells have been found to show good differentiation of acidic organelles such as lysosomes from other cellular compartments.

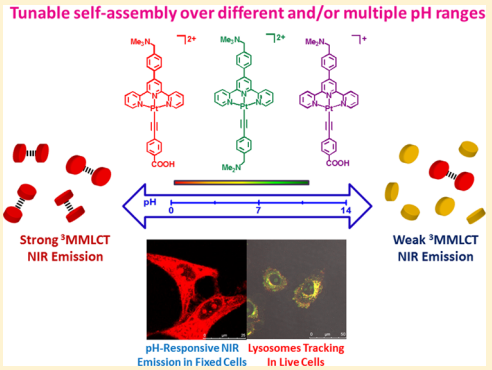

INTRODUCTION

The square-planar platinum(II) polypyridine complexes belong to a particularly interesting class of metal−ligand chromophoric complexes.[1−12] Apart from their rich spectroscopic and luminescence properties, they have been found to show a strong tendency to form highly ordered extended linear chains or oligomeric structures in the solid state.[1a−f,2,3b,c,4,6] With improvement in the solubility in organic solvents as well as in aqueous media, alkynylplatinum(II) terpyridine complexes have been demonstrated to undergo supramolecular self-assembly with d^8-d^8 metal−metal and/or $\pi-\pi$ interactions in both the solid and solution states.[5−12] With the help of noncovalent supramolecular interactions, different novel nanostructures have been constructed by this class of complexes.[4,7b,e,8,9] Moreover, the self-assembly process of the complexes can be readily modulated by the presence of external stimuli,[6−9] synthetic polyelectrolytes,[10,12] and biomolecules,[11,12] resulting in remarkable UV−vis absorption and emission spectral changes of the complexes. Such significant spectral changes have been utilized to detect important biomolecules,[11,12] their conformational changes,[11a,b] and their enzymatic activities.[11c,e]

Recently, water-soluble alkynylplatinum(II) terpyridine complexes have been reported to show interesting self-assembly and disassembly over physiological pH, leading to "switchable" near-infrared (NIR) emission both in solutions and in vitro.[7d] This allows the complexes to discriminate acidic organelles such as lysosomes from other cellular compartments in living cells. In addition, the applications of other phosphorescent platinum(II) complexes in bioimaging have been successfully demonstrated.[13] In view of the fact that NIR emission would be advantageous for fluorescence microscopy[14] and pH-responsive NIR luminescent probes are still relatively less explored in the literature,[15] we developed a new class of water-soluble pH-responsive alkynylplatinum(II) terpyridine complexes (Scheme 1) to extend the structural diversity and to have a better understanding on the structure−property relationship of the NIR-emissive complexes. The photophysical and electrochemical properties of the complexes were studied. Also, the induced self-assembly and disassembly processes of the

Received: March 1, 2016

DOI: 10.1021/acs.inorgchem.6b00513
Inorg. Chem. XXXX, XXX, XXX−XXX

Scheme 1. Chemical Structures of [Pt{tpy($C_6H_4CH_2NMe_2$-4)-4′}Cl](OTf) and Complexes 1−19

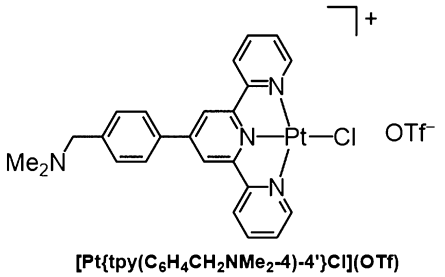

[Pt{tpy($C_6H_4CH_2NMe_2$-4)-4'}Cl](OTf)

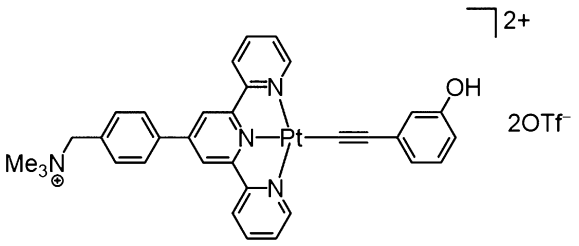

14

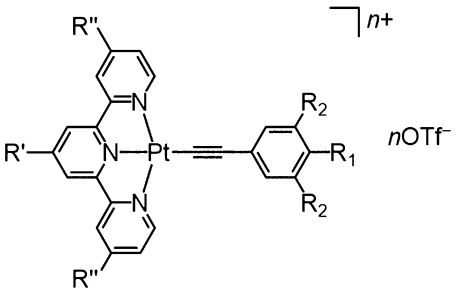

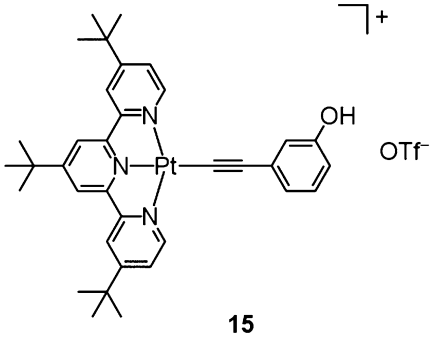

15

1: R′ = H, R″ = H, R_1 = CH_2NMe_2, R_2 = H, n = 1

2: R′ = H, R″ = H, R_1 = H, R_2 = CH_2NMe_2, n = 1

3: R′ = $C_6H_4CH_2\overset{\oplus}{N}Me_3$-4, R″ = H, R_1 = COOH, R_2 = H, n = 2

4: R′ = $C_6H_4CH_2\overset{\oplus}{N}Me_3$-4, R″ = H, R_1 = H, R_2 = CH_2NMe_2, n = 2

5: R′ = $C_6H_4CH_2\overset{\oplus}{N}Me_3$-4, R″ = H, R_1 = CH_2NMe_2, R_2 = H, n = 2

6: R′ = $C_6H_4CH_2\overset{\oplus}{N}Me_3$-4, R″ = H, R_1 = CH_2NH_2, R_2 = H, n = 2

7: R′ = $C_6H_4CH_2NMe_2$-4, R″ = H, R_1 = COOH, R_2 = H, n =1

8: R′ = $C_6H_4CH_2NMe_2$-4, R″ = H, R_1 = COOMe, R_2 = H, n =1

9: R′ = $C_6H_4CH_2NMe_2$-4, R″ = H, R_1 = H, R_2 = H, n =1

10: R′ = $C_6H_4CH_2NMe_2$-4, R″ = H, R_1 = $CH_2\overset{\oplus}{N}Me_3$-4, R_2 = H, n =1

11: R′ = *tert*-Butyl, R″ = *tert*-Butyl, R_1 = CH_2NMe_2, R_2 = H, n = 1

12: R′ = *tert*-Butyl, R″ = *tert*-Butyl, R_1 = H, R_2 = CH_2NMe_2, n = 1

13: R′ = *tert*-Butyl, R″ = *tert*-Butyl, R_1 = H, R_2 = OH, n = 1

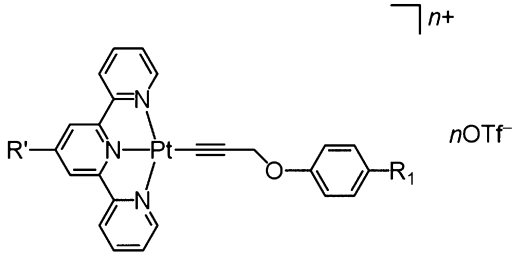

16: R′ = $C_6H_4CH_2\overset{\oplus}{N}Me_3$-4, R_1 = COOH, n = 2

17: R′ = $C_6H_4CH_2\overset{\oplus}{N}Me_3$-4, R_1 = OH, n = 2

18: R′ = $C_6H_4CH_2NMe_2$-4, R_1 = COOH, n = 1

19: R′ = $C_6H_4CH_2NMe_2$-4, R_1 = OH, n = 1

complexes in aqueous media as well as in vitro over different pH ranges were investigated.

RESULTS AND DISCUSSION

Synthesis and Characterization. Functionalized terpyridine (tpy) and alkynes were synthesized according to the synthetic pathways, as shown in Scheme S1 in the Supporting Information (SI). Synthetic details of specific functionalized ligands are included in the Experimental Section. The water-soluble chloroplatinum(II) terpyridine complex, [Pt{tpy($C_6H_4CH_2NMe_2$-4)-4′}Cl](OTf), was synthesized by the modification of a literature procedure for [Pt(tpy)Cl](OTf)[1a,2a,3a] using 4′-[4-(*N*,*N*-dimethylamino)methylphenyl]-2,2′:6′,2″-terpyridine instead of tpy, similar to the reported study of [Pt{tpy($C_6H_4CH_2NMe_3$-4)-4′}Cl](OTf)$_2$.[12] Both [Pt{tpy($C_6H_4CH_2NMe_2$-4)-4′}Cl](OTf) and [Pt{tpy($C_6H_4CH_2NMe_3$-4)-4′}Cl](OTf)$_2$ showed good solubility in water but only moderate solubility in common organic solvents such as dimethylformamide (DMF), methanol, and acetonitrile. The solubility of the platinum(II) complexes in common organic solvents was improved significantly after the coordination of alkynyl ligands by the dehydrohalogenation reaction of the chloroplatinum(II) complex with the corresponding functionalized alkynes in the presence of CuI as the catalyst in DMF and distilled triethylamine at room temperature under a N_2 atmosphere.[5,16] The identities of the chloroplatinum(II) precursor complex and all of the alkynylplatinum(II) terpyridine complexes, namely, **1**−**19**, were confirmed by ^{1}H NMR, IR spectroscopy, fast-atom-bombardment mass spectrometry (FAB-MS), and elemental analyses. Complexes **1**−**19** showed fairly strong absorptions at ca. 1153−1195 cm^{-1} and weaker absorptions at ca. 2103−2140 cm^{-1} in their IR spectra, which are in accordance with the presence of a trifluoromethanesulfonate counteranion and a σ-coordinated terminal alkynyl, respectively.

Electronic Absorption Spectroscopy. All of the complexes were soluble in acetonitrile or a mixture of acetonitrile, methanol, and/or dimethyl sulfoxide (DMSO) to give yellow to orange solutions with intense absorptions at ca. 260−343 nm and less intense lower-energy absorptions centered at ca. 399−

DOI: 10.1021/acs.inorgchem.6b00513
Inorg. Chem. XXXX, XXX, XXX−XXX

Table 1. Photophysical Data of Complexes 1−19

complex	medium (T/K)	electronic absorption λ/nm (ε/dm^3 mol^{-1} cm^{-1})	emission λ_{em}/nm (τ_0/μs)[a]	ψ_{lum}[b]
1	CH_3CN (298)	272 (29830), 281 (29960), 329 (11280), 340 (10060), 399 (2500), 423 (2160), 447 (1800)	607 (2.4), 735 (2.3)	2.6 × 10^{-3}
	solid (298)		783 (0.1)	
	solid (77)		900 (0.2)	
	glass[c] (77)		476[d] (13.2)	
2	CH_3CN (298)	286 (23270), 311 (10740), 328 (10540), 343 (11830), 426 (3960), 444 (3930)	591 (0.2)	4.5 × 10^{-4}
	solid (298)		784 (0.1)	
	solid (77)		894 (0.1)	
	glass[c] (77)		458[d] (11.5)	
3	CH_3CN (298)	272 (32020), 286 (33480), 321 (23380), 343 (18200), 402 (6140), 423 (5760), 535 sh (2120)	591 (0.2), 700 (0.1)	6.3 × 10^{-4}
	solid (298)		649 (0.1)	
	solid (77)		661 (0.5)	
	glass[c] (77)		480[d] (12.9)	
4	CH_3CN (298)	290 (38770), 327 (21590), 343 (11810), 430 (6110), 452 (5750)	608 (0.3), 715 (0.2)	1.6 × 10^{-3}
	solid (298)		695 (0.1)	
	solid (77)		719 (0.7)	
	glass[e] (77)		458[d] (11.5)	
5	CH_3CN (298)	276 (24600), 289 (23790), 310 (12400), 343 (6320), 420 (2470), 459 (2150)	619 (0.3), 725 (0.3)	1.9 × 10^{-3}
	solid (298)		794 (0.1)	
	solid (77)		907 (0.1)	
	glass[e] (77)		462[d] (9.6)	
6	CH_3CN (298)	274 (21400), 290 (23910), 306 (15230), 342 (7950), 425 (3560), 449 (3430)	625 (0.5)	4.4 × 10^{-3}
	solid (298)		770 (<0.1)	
	solid (77)		780 (0.3)	
	glass[e] (77)		498[d] (12.0)	
7	CH_3CN−CH_3OH (1:1, v/v) (298)	288 (28380), 327 (9560), 344 (7160), 425 (3400), 453 (3150)	613 (1.0), 700 (0.2)	2.5 × 10^{-3}
	solid (298)		683 (0.1)	
	solid (77)		713 (0.6)	
	glass[e] (77)		464[d] (10.1)	
8	CH_3CN (298)	291 (30390), 308 (21000), 337 (9590), 427 (4540), 453 (3690)	594 (0.2)	2.6 × 10^{-3}
	solid (298)		728 (0.1)	
	solid (77)		787 (0.5)	
	glass[e] (77)		491[d] (15.2)	
9	CH_3CN (298)	286 (22540), 308 (16150), 331 (12960), 380 (4110), 407 (4010), 456 (2010)	633 (0.5)	2.8 × 10^{-3}
	solid (298)		696 (0.1)	
	solid (77)		656 (0.6), 711 (0.6)	
	glass[e] (77)		511[d] (14.8)	
10	CH_3CN (298)	277 (39780), 292 (43960), 314 (29630), 336 (24650), 427 (3690), 446 (3200)	576 (0.2)	2.2 × 10^{-3}
	solid (298)		770 (0.1)	
	solid (77)		836 (0.1), 877 (0.1)	
	glass[e] (77)		499[d] (14.2)	
11	CH_3CN (298)	284 (45600), 310 (20990), 323 (19200), 338 (20670), 417 (6390), 426 (6230)	573 (0.5)	9.7 × 10^{-3}
	solid (298)		683 (0.1)	
	solid (77)		668 (0.2)	
	glass[c] (77)		466[d] (9.9)	
12	CH_3CN (298)	268 (50490), 284 (41430), 310 (20090), 323 (19240), 338 (21470), 418 (6550)	570 (0.5)	3.9 × 10^{-3}
	solid (298)		644 (0.1)	
	solid (77)		653 (0.3)	
	glass[c] (77)		459[d] (10.2)	
13	CH_3CN (298)	281 (55510), 310 (27710), 325 (27270), 339 (29080), 399 (7360), 427 (6850)	616 (0.1)	2.9 × 10^{-3}
	solid (298)		637 (0.1)	

DOI: 10.1021/acs.inorgchem.6b00513
Inorg. Chem. XXXX, XXX, XXX−XXX

Table 1. continued

complex	medium (T/K)	electronic absorption λ/nm (ε/dm^3 mol^{-1} cm^{-1})	emission λ_{em}/nm (τ_0/μs)[a]	ψ_{lum}[b]
	solid (77)		669 (0.2)	
	glass[c] (77)		464[d] (9.2)	
14	CH_3CN-CH_3OH (5:1, v/v) (298)	262 (39300), 290 (44020), 308 (26970), 331 (16820), 340 (14490), 418 (6970), 458 (6270), 550 sh (1330)	610 (0.3), 704 (0.2)	1.5×10^{-3}
	solid (298)		768 (0.1)	
	solid (77)		776 (0.2)	
	glass[c] (77)		489[d] (13.4)	
15	CH_3CN (298)	310 (34260), 329 (36720), 338 (31620), 391 (7900), 429 (5820)	610 (0.3)	9.4×10^{-3}
	solid (298)		638 (0.1)	
	solid (77)		647 (0.2)	
	glass[c] (77)		473[d] (10.4)	
16	CH_3CN-CH_3OH (5:1, v/v) (298)	275 (24060), 339 (3410), 415 (1440), 550 sh (450)	[f]	[f]
	solid (298)		669 (0.2)	
	solid (77)		675 (0.3)	
	glass[c] (77)		452[d] (11.1)	
17	CH_3OH–DMSO (30:1, v/v) (298)	273 (25360), 288 (24880), 324 (7640), 338 (6260), 404 (2460)	[f]	[f]
	solid (298)		669 (0.2)	
	solid (77)		714 (0.2)	
	glass[c] (77)		464[d] (9.3)	
18	CH_3CN-CH_3OH (5:1, v/v) (298)	260 (34060), 266 (33480), 287 (31800), 307 (18030), 322 (15790), 336 (14630), 416 (4640)	[f]	[f]
	solid (298)		687 (0.1)	
	solid (77)		711 (1.1)	
	glass[e] (77)		457[d] (15.2)	
19	CH_3CN-CH_3OH (5:1, v/v) (298)	272 (20580), 287 (21810), 309 (11820), 325 (9590), 337 (8510), 399 (3020), 410 (2910)	[f]	[f]
	solid (298)		689 (0.1)	
	solid (77)		588 (0.2), 702 (2.3)	
	glass[e] (77)		452[d] (10.6)	

[a]Emission lifetimes were recorded with ±10% uncertainty. [b]The luminescence quantum yield was measured at room temperature using $[Ru(bpy)_3]Cl_2$ as the standard. [c]In butyronitrile glass. [d]With vibrational progressional spacings of ca. 1250 cm^{-1}. [e]In acetonitrile–methanol–butyronitrile (4:1:100, v/v/v) glass. [f]Nonemissive.

480 nm. A summary of the electronic absorption spectral data of all of the complexes in solution has been tabulated in Table 1, and the electronic absorption spectra of representative complexes are shown in Figure S1 in the SI. The intense absorptions of the alkynylplatinum(II) terpyridine complexes **1**–**19** were assigned to the intraligand (IL) $\pi \rightarrow \pi^*$ transitions of the tpy and alkynyl ligands, with reference to previous spectroscopic work on related complexes.[5−12] On the other hand, because the lower-energy absorptions of the complexes with the same tpy ligand showed an energy trend that can be correlated to the electron richness of the alkynyl ligand, the absorptions probably originated from an admixture of dπ(Pt) $\rightarrow$ π^*(tpy) metal-to-ligand charge-transfer (MLCT) and alkynyl-to-tpy ligand-to-ligand charge-transfer (LLCT) transitions. For example, the lower-energy absorptions of the complexes with the 4′-[4-(*N*,*N*-dimethylamino)methylphenyl]-2,2′:6′,2″-terpyridine ligand in an acetonitrile solution showed an energy trend of **9** (λ_{max} = 456 nm) < **8** (453 nm) < **10** (446 nm) (Figure S1 in the SI). The energy trend could be rationalized by the presence of electron-withdrawing substituents on the phenyl ring of the alkynyl ligands in complexes **8** and **10**, which would, in turn, lower the energy level of the dπ(Pt) and π(C≡C–R) orbitals (HOMO). As a result, higher-energy absorptions, relative to the absorption of complex **9**, which contained an unsubstituted ethynylphenyl ligand, were observed in complexes **8** and **10**.

It would be worth noting that complexes **3** and **14** in acetonitrile and/or methanol solution mixtures displayed low-energy absorption shoulders at ca. 550 nm (Table 1). On the basis of the previous spectroscopic work on alkynylplatinum(II) terpyridine complexes,[6−12] the lower-energy absorption shoulders should be attributable to a metal–metal-to-ligand charge-transfer (MMLCT) transition, due to the intermolecular aggregation of the complex molecules with Pt···Pt and/or π–π interactions. The ground-state aggregation of complex **3** in an aqueous solution (50 mM NaCl) at pH 2 was further investigated by concentration-dependent UV–vis absorption studies. The results showed that the low-energy absorption tail at 700 nm did not obey Beer's law (Figure 1), indicative of the self-aggregation of complex **3** molecules in the pH 2 aqueous solution at high concentrations. This self-aggregation occurred presumably through Pt···Pt and/or π–π interactions, leading to the observation of low-energy MMLCT absorption.

Emission Spectroscopy. Upon excitation at $\lambda_{ex} \geq 400$ nm, all of the complexes, except complexes **16**–**19**, showed emissions in degassed solutions (Figure S2 in the SI). The emission data of complexes **1**–**19** in solution, their luminescence quantum yields, and their solid- and glass-state emissions have been summarized in Table 1. For the emissions

DOI: 10.1021/acs.inorgchem.6b00513
Inorg. Chem. XXXX, XXX, XXX–XXX

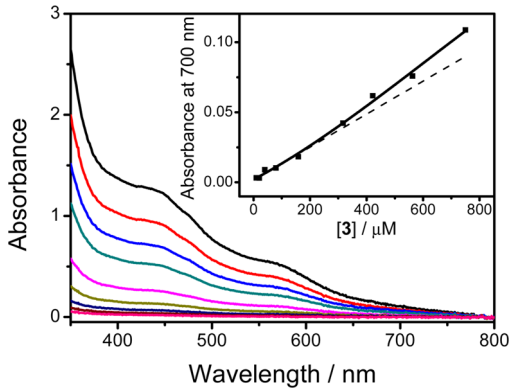

Figure 1. Concentration-dependent UV−vis absorption spectra of complex **3** in an aqueous solution (50 mM NaCl) at pH 2 at 298 K. Apparent absorbance refers to the absorbance value corrected to 1-cm-path-length equivalence. Inset: Plot of the absorbance at 700 nm against the concentration of complex **3**.

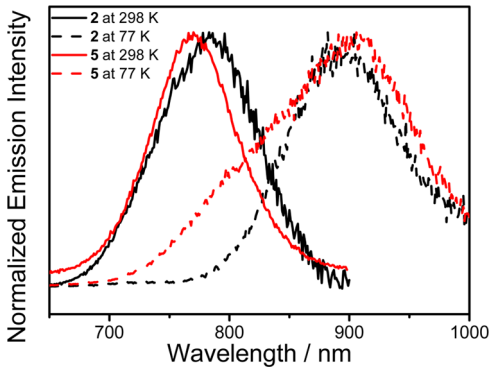

Figure 2. Emission spectra of complexes **2** and **5** in the solid state at 298 and 77 K.

located at ca. 573−654 nm, their lifetimes were found to be in the microsecond range. Together with their large Stokes shifts and our previous spectroscopic studies of alkynylplatinum(II) terpyridine complexes,[5−12] the emissions were tentatively assigned as derived from admixtures of triplet metal-to-ligand charge-transfer (^{3}MLCT; $^3[d\pi(Pt)\rightarrow\pi^*(tpy)]$) and triplet ligand-to-ligand charge-transfer (^{3}LLCT; $^3[\pi(C{\equiv}C{-}R)\rightarrow\pi^*(tpy)]$) excited states. This assignment was further supported by the excitation spectra of the complexes monitored at their emission maxima in solutions, with representative spectra shown in Figures S3−S6 in the SI. The excitation maxima of these complexes were found to be in the same region as the MLCT/LLCT absorptions of the complexes in the solution state. Also, the observation of the energy trend of **9** (λ_{em} = 633 nm) < **7** (613 nm) < **8** (594 nm) is in accordance with the charge-transfer (CT) assignment. The higher-energy ^{3}MLCT/^{3}LLCT emissions of complexes **7** and **8** were ascribed to the presence of the electron-withdrawing substituent on the aryl group of the alkynyl ligands, which would lower the energy level of the dπ(Pt) and π(C≡C−R) orbitals (HOMO), resulting in an increase in the CT energy compared to that of **9**.

In addition to the ^{3}MLCT/^{3}LLCT emission, complexes **1**, **3**, **4**, **7**, and **14** were found to be dual-emissive, with a lower-energy emission band centered at ca. 700−735 nm. The excitation spectra of complexes **1** and **4** monitored at these low-energy emissions (Figure S3 in the SI) revealed a larger contribution in the lower-energy region than their MLCT/LLCT absorptions in the solution state. Together with the fact that complex **3** underwent ground-state aggregation and showed low-energy MMLCT absorption in aqueous solutions (Figure 1), the low-energy emissions of these complexes were probably derived from excited states of a triplet metal−metal-to-ligand charge-transfer (^{3}MMLCT) origin, due to aggregation of the complex molecules in the solution state with Pt···Pt and/or π−π interactions.

The solid-state emissions of the complexes at 298 K were observed at ca. 637−794 nm (Figure 2). The excitation spectral features monitored at the solid-state emission maxima of the complexes were found to occur at lower energy compared to their solution-state absorption. The emissions should originate from ^{3}MMLCT excited states due to the formation of Pt···Pt and/or π−π interactions in the solid lattice. With the exception of complex **11**, the solid-state emissions of the complexes at 77 K occurred at much lower energy than those at 298 K (Figure 2). This could be accounted for by the lattice contraction of the complexes at low temperatures, resulting in stronger Pt···Pt and π−π interactions and hence lower-energy ^{3}MMLCT emissions. On the other hand, the glass-state emissions of all of the complexes at 77 K showed intense and highly structured emissions from 452 to 517 nm (Figure S7 in the SI), with vibrational progressional spacings of ca. 1250 cm^{-1}, which were typical of the vibrational stretching frequencies of aromatic C=C and C=N modes. In view of the long emission lifetimes (in the microsecond range), the emissions were tentatively assigned as metal-perturbed ^{3}IL emission of the tpy ligand, with mixing of a ^{3}MLCT/^{3}LLCT state.

Electrochemical Studies. The cyclic voltammograms of all of the complexes were recorded in DMF in the presence of 0.1 M ^{n}Bu$_4$NPF$_6$ as the supporting electrolyte. The reductions of the complexes were found to be insensitive to the nature of the alkynyl ligands but related to the substituent on the tpy ligands, where more negative potentials were found in the complexes with a *tert*-butyl-substituted tpy ligand and less negative potentials were observed in the complexes with unsubstituted tpy, 4′-[4-(trimethylamino)methylphenyl]-2,2′:6′,2″-terpyridine, and 4′-[4-(*N*,*N*-dimethylamino)methylphenyl]-2,2′:6′,2″-terpyridine. All of the electrochemical data are summarized in Table S1 in the SI, and the cyclic voltammograms for the oxidation and reduction of the representative complexes are depicted in Figures S8−S10 in the SI. The reduction couples were tentatively assigned as one-electron reductions of the tpy ligands of the complexes. The more negative reduction potentials of the complexes with a *tert*-butyl-substituted tpy ligand are in line with the electron-donating properties of the three *tert*-butyl groups, leading to a rise in the π^* orbital, which is the LUMO. On the other hand, the additional aryl groups on the 4′-[4-(trimethylammonium)-methylphenyl]-2,2′:6′,2″-terpyridine and 4′-[4-(*N*,*N*-dimethylamino)methylphenyl]-2,2′:6′,2″-terpyridine ligands in complexes **3**−**10**, **14**, and **16**−**19** should not be perfectly coplanar with the tpy ligand because of steric repulsion.[16] Therefore, these complexes have lower-lying π^* orbitals and showed less negative reduction potentials compared to the complexes with *tert*-butyl-substituted tpy (**11**−**13** and **15**; Table S1 in the SI).

In addition to the two quasi-reversible reduction couples, the complexes with 4′-[4-(trimethylammonium)methylphenyl]-2,2′:6′,2″-terpyridine and 4′-[4-(*N*,*N*-dimethylamino)-methylphenyl]-2,2′:6′,2″-terpyridine displayed an additional irreversible cathodic reduction wave at E_{pc} = −1.23 to −1.25

DOI: 10.1021/acs.inorgchem.6b00513
Inorg. Chem. XXXX, XXX, XXX−XXX

V and −0.96 to −0.99 V versus saturated calomel electrode (SCE), respectively. With reference to the reductions of the free 4′-[4-(trimethylammonium)methylphenyl]-2,2′:6′,2″-terpyridine trifluoromethanesulfonate ligand (where an irreversible cathodic reduction wave at E_{pc} = −1.46 V vs SCE was found) and the reported amine-substituted molecules,[17] the irreversible reductions should be attributable to (aminomethyl)benzene-based reductions of the substituted tpy ligands.

All of the alkynylplatinum(II) terpyridine complexes showed an irreversible anodic oxidation wave at E_{pa} = +0.96 to +1.38 V vs SCE, which is sensitive to the electron richness of the alkynyl ligand and the platinum(II) metal center. For complexes **3**, **7**, and **8**, which contain a strongly electron-withdrawing carboxyl or carboxylate group on the phenyl ring of the alkynyl ligands, the potentials of their oxidation waves were found to be more positive. This suggests that the oxidation should originate from a metal-centered/alkynyl-ligand-centered oxidation, typical of alkynylplatinum(II) terpyridine complexes.[3c,f,g,5,7d] The electron-withdrawing substituent on the alkynyl ligand would lower the dπ(Pt) and π(C≡C−R) orbitals, resulting in reduced ease of oxidation of the complexes and more positive potentials in complexes **3**, **7**, and **8**. For the complexes containing 4′-[4-(*N*,*N*-dimethylammonium)methylphenyl]-2,2′:6′,2″-terpyridine ligands (**7**−**10**, **18**, and **19**), reversible oxidation couples were found at $E_{1/2}$ = +0.41 to +0.42 V vs SCE, which were tentatively assigned as (aminomethyl)benzene-based oxidations, similar to the reversible oxidation of amine-containing molecules reported in the literature.[18]

Induced Self-Assembly/Disassembly in Aqueous Solutions at Different pHs. Dynamic light scattering (DLS) experiments have been conducted to provide a better understanding of the self-assembly process of complex **3** at different pHs. A number-averaged hydrodynamic diameter (D_h) of ca. 1.8 μm was found in a pH 2 aqueous solution of complex **3**, while particles of smaller size of ca. 1.5 μm with lower signal intensity were observed in a pH 7 solution (Figure S11 in the SI). In addition, much smaller particles of ca. 300 nm were found in a pH 7 aqueous solution of complex **3**. The observation of micron-sized particles in the DLS experiments supports the self-assembly of complex **3** molecules, presumably through Pt···Pt and/or π−π interactions. This is in accordance with the results of the concentration-dependent UV−vis absorption study (Figure 1). An increase in the pH from 2 to 7 resulted in a decrease in D_h as well as the signal intensity of the large particles. Together with the finding of smaller particles in a pH 10 solution, this indicates the lower degree of aggregation of complex **3** molecules in aqueous solutions at higher pHs. Modulation of the self-assembly process of complex **3** by pH changes should originate from deprotonation of the pH-responsive −COOH moiety on complex **3** at higher pHs, resulting in an increase in the hydrophilicity of the complex and hence the occurrence of deaggregation.

Further investigations on the self-assembly process of the platinum(II) complexes were carried out by UV−vis absorption and emission studies of the complex in aqueous solutions at different pHs. Because complexes **1**−**19** contain different pH-responsive groups that should have different pK_a and pK_a* values, spectroscopic measurements were carried out over different pH ranges. For example, both complexes **2** and **4** contain the pH-responsive $-CH_2NMe_2$ group. Upon an increase in the pH, both the aqueous solutions of **2** and **4** showed a decrease in higher-energy MLCT/LLCT absorptions at ca. 396 and 425 nm, respectively, with concomitant growth of the absorption shoulders at ca. 500 and 550 nm. Their UV−vis absorption spectra in aqueous solutions (50 mM NaCl) at different pHs are shown in Figures 3 and S12−S15 in the SI.

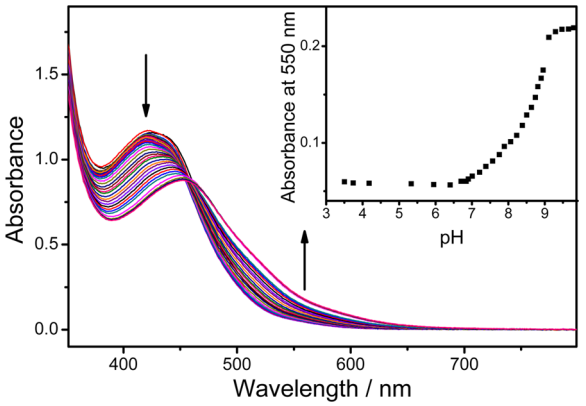

Figure 3. Electronic absorption spectra of complex **4** (200 μM) in an aqueous solution (50 mM NaCl) at different pHs. Inset: Plot of the absorbance of complex **4** at 550 nm versus pH.

The electronic absorption spectra of complex **4** were also found to be sensitive to the temperature of the solution, with a significant decrease in the absorption shoulder at 550 nm and growth of MLCT/LLCT absorption at higher temperatures (Figures S14 and S15 in the SI). The temperature-dependent low-energy absorption shoulder and the high reversibility of the absorptions over seven cycles of heating and cooling indicated the self-assembly of complex molecules in aqueous solutions at room temperature,[7a−c,e,8] and the absorption shoulder was tentatively assigned as an MMLCT absorption, presumably through Pt···Pt and/or π−π interactions. Because an increase in the MMLCT absorption of complexes **2** and **4** were observed at high pH values, this suggested an enhanced aggregation of the complex molecules at high pHs, which can be explained by deprotonation of the positively charged $-CH_2NHMe_2^+$ groups of complexes **2** and **4** upon an increase in the pH of the aqueous solutions, resulting in a decrease in the overall hydrophilicity and a decrease in the electrostatic repulsion among the platinum(II) complex molecules (Figures 3 and S12 in the SI). On the basis of the electronic absorption spectral changes at different pHs, the pK_{a1} and pK_{a2} of complex **4** were determined to be 7.81 and 8.84, respectively (Figures 3 and S13 in the SI).[15b,d−h] On the other hand, because of the lower solubility of the complex **2** molecules at higher pHs, complex **2** was found to precipitate out from the aqueous solution at around pH 8 (no precipitation of complex **4** was found because of the presence of water-solubilizing $-CH_2NMe_3^+$ group on the tpy ligand), and hence the pK_a value(s) of complex **2** could not be determined.

At high pHs, complexes **2** and **4** were found to emit in the NIR region upon excitation at 457 and 431 nm (the isosbestic wavelengths of the electronic absorption spectra of the complexes with different pHs), respectively (Figures 4 and S16 and S17 in the SI). Also, the NIR emissions of aqueous solutions of **4** at both pH 4 and 10 showed a significant decrease in the emission intensity with increasing temperature (Figures S18 and S19 in the SI). The almost complete "turn-off" of the NIR emission of complex **4** at pH 4 suggested that the decrease in the NIR emission intensity cannot be solely due to more efficient nonradiative decay at higher temperatures.

DOI: 10.1021/acs.inorgchem.6b00513
Inorg. Chem. XXXX, XXX, XXX−XXX

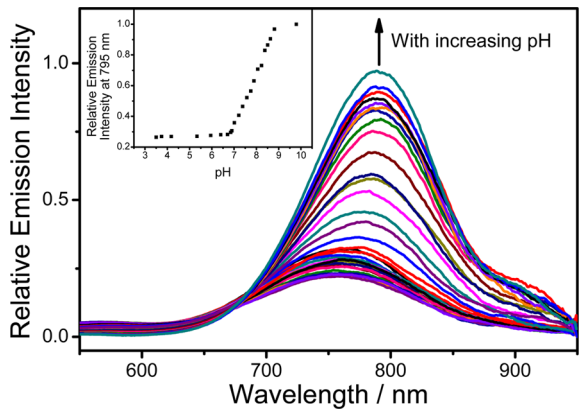

Figure 4. Emission spectra of complex **4** (200 μM) in an aqueous solution (50 mM NaCl) at different pHs. Excitation was at 431 nm. Inset: Plot of the relative emission intensity of complex **4** at 795 nm versus pH.

This, together with the observation of a higher-energy emission at ca. 578 nm of complex **4** at higher temperatures (Figure S18 in the SI), indicated the self-assembly of complex molecules at room temperature, which is in agreement with the results of the UV−vis absorption measurements. The aggregated complex molecules through Pt···Pt and/or π−π interactions would emit in the NIR region of ^{3}MMLCT character upon excitation, while higher temperatures favored deaggregation of the complex molecules, leading to (1) a decrease in the ^{3}MMLCT emission intensity and (2) growth of the ^{3}MLCT/^{3}LLCT emission at ca. 578 nm originating from the monomeric complex molecules (Figures S18 and S19 in the SI).

A decrease in the pH values of the solutions of complexes **2** and **4** revealed a decrease in the ^{3}MMLCT emission intensity, with a blue shift in the emission maxima and a growth of higher-energy ^{3}MLCT/^{3}LLCT emissions (Figures 4 and S16 in the SI). This can be rationalized by protonation of the $-CH_2NMe_2$ groups on the alkynyl ligands of the complexes, which would lead to an increase in the overall hydrophilicity of complexes **2** and **4** and an increase in the electrostatic repulsion among the platinum(II) complex molecules. Therefore, deaggregation of the complex molecules would occur, resulting in a decrease in the ^{3}MMLCT emission intensity and a blue shift in emission maxima (Figures 4 and S16 in the SI). These changes in emission of complex **4** at different pHs would allow determination of the pK_{a1}* and pK_{a2}* values. These values were determined to be 7.62 and 8.42, respectively (Figure S17 in the SI); the small discrepancy between the pK_{a1} and pK_{a2} and the pK_{a1}* and pK_{a2}* values could be explained by the small difference in the basicity of the complex molecules in the ground and excited states.

An attempt was made to incorporate two different pH-responsive groups, $-CH_2NMe_2$ and −COOH, which should have significant difference on the pK_a* value from each other, into the alkynylplatinum(II) terpyridine moieties, and complex **7** was synthesized. Before the emission properties of complex **7** were studied at different pHs, the pH response of another platinum(II) complex containing the −COOH group, complex **3**, was investigated by UV−vis absorption and emission measurements (Figures S20 and S21 in the SI). It was found that the electronic absorption spectra of complex **3** showed a red shift with increasing pH (Figure S20 in the SI), similar to the reported study on alkynylplatinum(II) terpyridine complexes containing phenolic proton(s).[7d] This can be explained by deprotonation of the carboxylic group on the alkynyl ligand of complex **3** at higher pHs, leading to an increase in the electron richness of the alkynyl ligand of complex **3**. This results in an increase in the energy level of the dπ(Pt) and π(C≡C−R) orbitals and hence gives rise to a red shift of both the MLCT/LLCT and MMLCT absorptions. On the other hand, the emission spectra of the aqueous solution of complex **3** revealed a decrease in the intensity of ^{3}MMLCT emission centered at 760 nm with increasing pH, and the pK_a* value of complex **3** deduced from the emission spectra was determined to be 2.51 (Figure S21 in the SI). This could be ascribed to the increase in the hydrophilicity of the complex after deprotonation of the carboxylic proton, resulting in deaggregation of the complex molecules. Also, more effective PET would be likely to occur after deprotonation of the −COOH group at higher pHs. On the basis of deaggregation of the complex molecules and the more effective PET quenching, a significant decrease in the NIR emission of complex **3** was observed at high pHs (Figure S21 in the SI).

In view of the significant difference in the pK_a* values of the −COOH and $-CH_2NHMe_2^+$ groups, the photophysical properties of complex **7** in aqueous solutions at different pHs were investigated (Figures 5 and S22 and S23 in the SI). The electronic absorption spectrum of the aqueous solution of complex **7** (200 μM) at pH 1.62 showed a high-energy absorption at ca. 456 nm and a lower-energy absorption band at ca. 576 nm (Figure S22 in the SI), which would originate from the MLCT/LLCT and MMLCT transitions, typical of

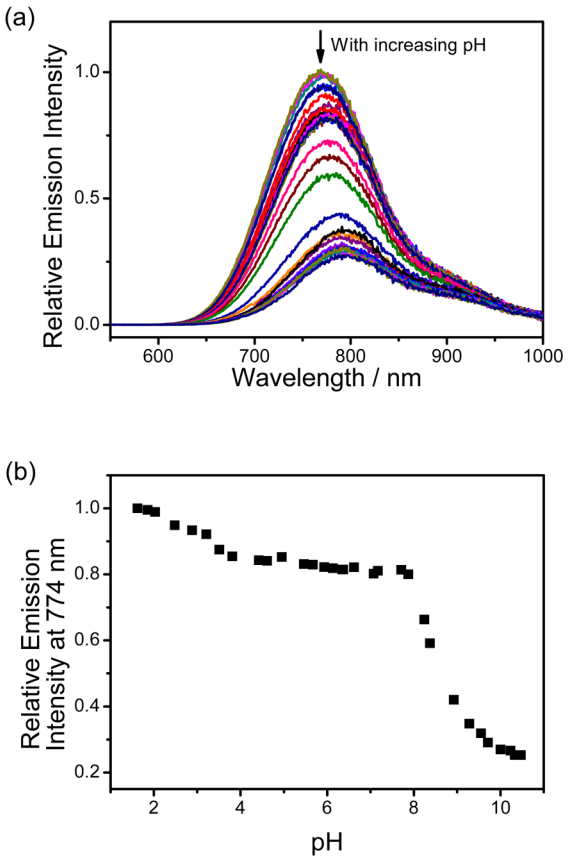

Figure 5. Emission spectra of complex **7** (200 μM) in an aqueous solution (50 mM NaCl) at different pHs. Excitation was at 456 nm. Inset: Plot of the relative emission intensity of complex **7** at 760 nm versus pH.

DOI: 10.1021/acs.inorgchem.6b00513
Inorg. Chem. XXXX, XXX, XXX−XXX

alkynylplatinum(II) terpyridine complexes.[5−12] Upon an increase in the pH from 1.62 to 4.95, there was a drop in the absorptions at ca. 456 and 576 nm, while an increase in the absorptions at ca. 506 and 650 nm was found (Figure S22 in the SI), similar to the electronic absorption spectral changes of complex **3** upon an increase in the pH of the aqueous solution. Therefore, the spectral changes of complex **7** would likely be due to deprotonation of the −COOH group on the alkynyl ligand, leading to an increase in the electron richness of the alkynyl ligand and an increase in the energy levels of the dπ(Pt) and π(C≡C−R) orbitals. As a result, a decrease in the CT energy and a red shift in the MLCT/LLCT and MMLCT absorptions were observed, giving rise to an increase in absorbance at 506 and 650 nm from pH 1.6 to 5.0 (Figure S22 in the SI).

After passing through pH 4.95, the absorption of the aqueous solution of complex **7** remained almost unchanged with increasing pH up to 8.37. A further increase in the pH above 8.37 revealed another increase in the absorption at ca. 650 nm with a drop in the absorptions at ca. 456 and 576 nm (Figure S22 in the SI). Because the −COOH group on the alkynyl ligand of complex **7** should undergo deprotonation at much lower pHs (as suggested by the pK_a* value of complex **3**, which was found to be 2.51; Figure S21 in the SI), it is unlikely that the UV−vis absorption spectral changes of complex **7** above pH 8.37 were related to the −COOH group. In view of the electronic absorption spectra of complex **4** at high pHs (Figure 2), the increase in the absorption of complex **7** at 650 nm can be explained by the growth of MMLCT absorption due to deprotonation of the $-CH_2NHMe_2^+$ group on the tpy ligand. This would lead to a decrease in the hydrophilicity of the complex molecules and hence an enhanced aggregation with Pt···Pt and/or $\pi-\pi$ interactions. As a result, significant changes in the absorption of complex **7** at 650 nm were found at both low and high pHs (Figure S22 in the SI), which would be ascribed to the red shift upon deprotonation of the −COOH group and enhanced aggregation by deprotonation of the $-CH_2NHMe_2^+$ group, respectively.

Similar to its UV−vis absorption behavior, the emission properties of complex **7** in an aqueous solution can also be modulated by pH changes at two distinguishable regions, as shown in Figure 5. Upon excitation at 468 nm, the aqueous solution of complex **7** at pH 1.62 was found to emit at ca. 774 nm, originating from the ^{3}MMLCT state due to aggregation of complex molecules with Pt···Pt and/or $\pi-\pi$ interactions.[6−12] The emission intensity decreased from pH 1.62 to 4.54, followed by almost a leveling off until pH 7.71 and then a significant drop from pH 7.71 to 10.47. In addition, a red shift in the emission maximum was observed at pH above 8.30, with λ_{em} = 800 nm at pH 10.47 (Figure 5). With reference to the UV−vis absorption and emission spectral changes of the pH-responsive platinum(II) complexes mentioned above, the decrease in the NIR emission intensity of complex **7** from pH 1.62 to 4.54 was probably due to deprotonation of the −COOH group on the alkynyl ligand. This would increase the hydrophilicity of the complex molecules and lead to deaggregation. Together with the increase in electron richness of the alkynyl ligand and hence likely a more effective PET quenching after deprotonation of the −COOH group, the first drop in the ^{3}MMLCT emission intensity was observed over pH 1.62−4.54. Because deprotonation of the −COOH group should be almost complete at pH 4.54, a further increase in the pH would not result in significant changes in the degree of PET quenching as well as the hydrophilicity of complex **7** and its aggregation. This would account for the small changes in the emission intensity from pH 4.54 to 7.71. On the other hand, at pH above 7.71, deprotonation of the positively charged $-CH_2NHMe_2^+$ group on the tpy ligand of complex **7** would likely occur, as supported by the electronic absorption spectra of complex **7** (Figure S22 in the SI). As a result, a more effective PET quenching would contribute to the significant decrease in the NIR emission intensity from pH 7.71 to 10.47 (similar findings of PET quenching of luminophores by tertiary amines have been reported[19]). It is worth noting that an obvious red shift in the emission maximum was found at pH above 8.30 (Figure 5). This, together with the growth of MMLCT absorption observed in the electronic absorption spectra of complex **7** at high pHs (Figure S22 in the SI), suggested an enhanced aggregation of the complex molecules at high pHs. However, probably because of the more effective PET quenching, the ^{3}MMLCT emission showed a drop, instead of an increase, in the emission intensity. The pK_{a1}* and pK_{a2}* values of complex **7**, which corresponded to the acid dissociation constant of −COOH and the positively charged $-CH_2NHMe_2^+$ groups on complex **7**, were determined to be 3.26 and 8.53, respectively (Figure S23 in the SI).

The emission lifetimes of representative complexes in aqueous solution (50 mM NaCl) were measured (Table S2 in the SI) in order to investigate the effect of dissolved oxygen on the emission properties of the complexes. Because the lifetimes of the ^{3}MMLCT emissions of the complexes were smaller than 0.1 μs, no significant changes in the emission intensity of the complexes (<1.6%) were anticipated by a change in the dissolved oxygen concentration of 1 mg L^{-1} at 25 °C (for details, refer to the Experimental Section). This suggests that the platinum(II) complexes are good reporters of pH changes in aqueous solutions based on their self-assembly/disassembly properties and ^{3}MMLCT emissions in the NIR region.

Fixed-Cell Imaging Experiments at Different Intracellular pHs by the NIR Emission of Complex 3. To further demonstrate the potential application of this class of complexes as NIR luminescent probes in vitro, the pH response of the ^{3}MMLCT emission of complex **3** was investigated using HeLa cells fixed with methanol. Methanol fixation can result in the precipitation of proteins and removal of lipids from cells, as well as permeable membranes.[20] As a result, any observable change in the ^{3}MMLCT emission intensity will not be due to the binding of complex **3** to proteins/biomolecules or different concentrations of complex **3** in cellular compartments. Confocal microscopy images of fixed HeLa cells incubated with complex **3** (20 μM) in serum- and phenol-red-free Dulbecco's modified Eagle's medium (DMEM) at 37 °C for 1 h,[21] followed by further incubation in pH 2.00 and 7.09 2-(*N*-morpholino)ethanesulfonic acid (MES) buffer solutions at room temperature for 10 min, revealed a strong NIR emission at λ_{em} = 750 ± 50 nm and a very weak emission, respectively (Figure 6). Because fixed cells have permeable membranes,[20] the intracellular pH should be equal to the pH value of the buffer solution, suggesting that the NIR emission intensity is closely associated with the intracellular pH environment. Therefore, it is likely that complex **3** will undergo self-assembly and show strong NIR emission in fixed cells at low pHs. However, at higher pHs, deprotonation of the −COOH group would lead to an increase in the hydrophilicity and the

DOI: 10.1021/acs.inorgchem.6b00513
Inorg. Chem. XXXX, XXX, XXX−XXX

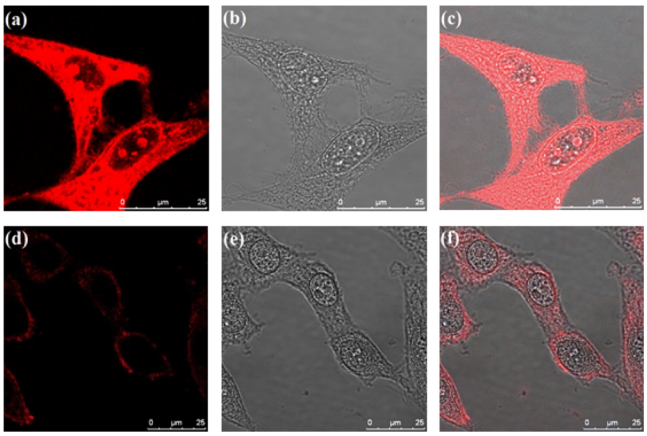

Figure 6. (a and d) Luminescence, (b and e) bright-field, and (c and f) overlaid images from confocal microscopy of fixed HeLa cells incubated with complex **3** (20 μM) for 1 h followed by incubation with buffer solutions of pH (a–c) 2.00 or (d–f) 7.09 at room temperature for 10 min. λ_{ex} = 488 nm and λ_{em} = 750 ± 50 nm.

disassembly of complex molecules, resulting in a decrease in the ^{3}MMLCT emission intensity (Figure 6).

Live-Cell Imaging Experiments by the NIR Emission of Complex 7. On the basis of the pH-responsive NIR emissions of the platinum(II) complexes in fixed cells, it is conceivable that the complexes can be utilized for probing cellular organelles, such as lysosomes, that show significant deviation of the pH values from physiological pH (7.0–7.4) in live cells. Confocal microscopy images of live HeLa cells incubated with complex **7** (16 μM) in serum- and phenol-red-free DMEM at 37 °C for 1 h are shown in Figure 7. Different intensities of

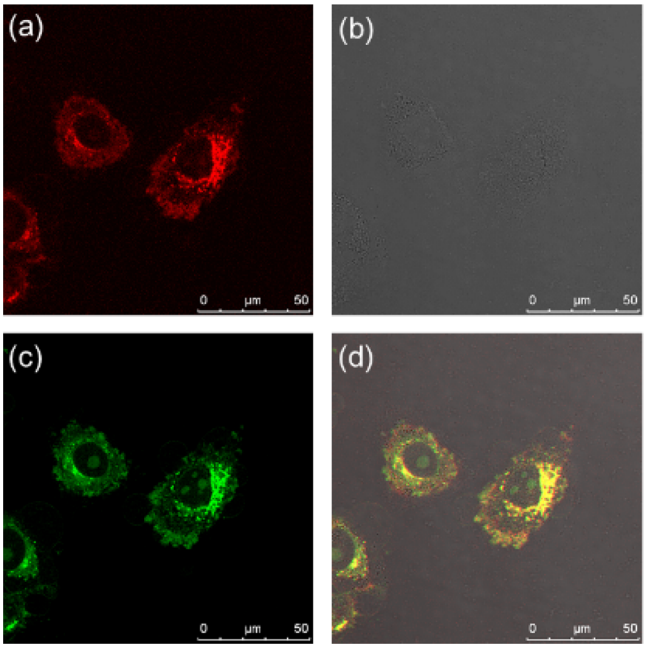

Figure 7. Confocal microscopy images of live HeLa cells incubated with complex **7** (16 μM) for 1 h, followed by incubation with DND-189 (1 μM) in serum- and phenol-red-free DMEM for 15 min. λ_{ex} = 488 nm. (a) Luminescence image at λ_{em} = 750 ± 50 nm, (b) bright-field image, (c) luminescence image at λ_{em} = 525 ± 25 nm from the costained DND-189, and (d) the merged image of the emissions at λ_{em} = 750 ± 50 and 525 ± 25 nm are shown in the corresponding figures.

NIR emissions at λ_{em} = 750 ± 50 nm were observed in different cellular compartments, with stronger emissions found in vesicular distribution (Figure 7a). Such strong NIR emissions showed good colocalization with the green emission of the costained LysoSensor Green DND-189 (Figure 7c), as indicated from the yellow spots in the merged images (Figure 7d).[22] Because DND-189 is known to accumulate and show stronger green emission in acidic organelles such as lysosomes, the good colocalization of the strong NIR emission of complex **7** suggests that this complex would emit more strongly in an acidic environment, probably owing to the enhanced self-assembly and less efficient PET quenching at low pHs. This demonstrates the potential of complex **7** to differentiate organelles (such as lysosomes) with pH values significantly different from those of the other cellular compartments, in live cells by the pH-responsive ^{3}MMLCT emission in the NIR region.

CONCLUSIONS

A new class of water-soluble pH-responsive alkynylplatinum(II) terpyridine complexes was successfully synthesized and characterized. The photophysical and electrochemical properties of the complexes were studied. Most of the complexes exhibited rich luminescence properties in solid and solution states, and some of them were found to undergo self-assembly with Pt···Pt and/or π–π interactions in solutions, resulting in ^{3}MMLCT emission in the NIR region. The self-assembly processes of complexes **2**–**4** and **7** can be modulated readily by pH changes, owing to the changes in the hydrophilicity of the complexes upon protonation/deprotonation of the pH-responsive groups. Together with the changes in the electrostatic repulsion among the complex molecules or the extent of PET quenching upon protonation/deprotonation, complexes **3** and **4** were found to show remarkable UV–vis absorption and emission spectral changes over pH 1.6–5.0 and 6.8–8.5, respectively. For complex **7**, which contains both –COOH and $-CH_2NHMe_2^+$ groups with different pK_a* values (3.26 and 8.53, respectively), interesting two-step changes in the ^{3}MMLCT emission intensity in the NIR region were observed over two distinguishable pH regions. In vitro cell-imaging experiments of complex **3** revealed a pH-responsive ^{3}MMLCT emission in the NIR region from fixed HeLa cells, while complex **7** was capable of differentiating cellular organelles of different pH values based on its pH-responsive ^{3}MMLCT emission in live HeLa cells.

EXPERIMENTAL SECTION

Materials and Reagents. 2-Acetylpyridine, *p*-tolualdehyde, 2,2′-azobis(2-methylpropionitrile) (AIBN), methyl 4-iodobenzoate, ethyl 4-iodobenzoate, 4-iodotoluene, trimethylamine (33 wt % in ethanol), dimethylamine (2.0 M in methanol), 1-iodo-3,5-dimethylbenzene, ethyl 4-hydroxybenzoate, hydroquinone, and ethyl bromoacetate were purchased from Sigma-Aldrich. (Trimethylsilyl)acetylene was purchased from GFS Chemicals. Propargyl bromide (80% in toluene solution by weight) was purchased from Acros Organics Company. Dulbecco's modified Eagle's medium (DMEM), fetal bovine serum (FBS), phosphate-buffered saline at pH 7.2 (PBS), trypsin–ethylenediaminetetraacetic acid, and penicillin/streptomycin were purchased from Invitrogen. 4′-(*p*-Tolyl)-2,2′:6′,2″-terpyridine,[23] 4′-[4-(bromomethyl)phenyl)]-2,2′:6′,2″- terpyridine,[24] 1-ethynyl-3,5-benzenedimethanol,[25] 1-ethynyl-3,5-bis(*N*,*N*-dimethylamino)benzene,[26] [HC≡C$C_6H_4CH_2NMe_3$-4](OTf),[10b] methyl 4-ethynylbenzoate,[26] 4-(propargyloxy)benzoic acid,[27] and 4-(propargyloxy)phenol[28] were synthesized according to the reported literature. [Pt(tpy)Cl](OTf)

DOI: 10.1021/acs.inorgchem.6b00513
Inorg. Chem. XXXX, XXX, XXX–XXX

and [Pt(*t*Bu$_3$tpy)Cl](OTf) were synthesized by modification of a literature method.[1a,2a,3a] [(Trimethylamino)methylphenyl]-2,2′:6′,2″-terpyridine trifluoromethanesulfonate, [Pt{tpy(C$_6$H$_4$CH$_2$NMe$_3$-4)-4′}Cl](OTf)$_2$, and [Pt{tpy(C$_6$H$_4$CH$_2$NMe$_3$-4)-4′}(C≡CC$_6$H$_5$)](OTf)$_2$ were synthesized as reported previously.[12] All other reagents were of analytical grade and were used without further purification. The reactions were performed under an inert atmosphere of N_2 unless specified otherwise.

Physical Measurements and Instrumentation. ^{1}H NMR spectra were recorded with a Bruker AVANCE 400 (400 MHz) or a Bruker DPX-300 (300 MHz) Fourier transform NMR spectrometer at ambient temperature with tetramethylsilane (Me_4Si) as an internal reference. Positive-ion FAB-MS or electron impact mass spectrometry (EI-MS) spectra were recorded on a Thermo Scientific DFS High Resolution Magnetic Sector mass spectrometer, while positive and negative electrospray ionization mass spectra were recorded on a Finnigan LCQ spectrometer. Elemental analyses for the metal complexes were performed on a Carlo Erba 1106 elemental analyzer at the Institute of Chemistry, Chinese Academy of Sciences, Beijing, China. IR spectra of the solid samples were obtained as Nujol mulls on KBr disks on a Bio-Rad FTS-7 Fourier transform infrared spectrophotometer (4000−400 cm^{-1}). UV−vis absorption spectra were recorded on a Cary 50 (Varian) spectrophotometer equipped with a xenon flash lamp. Steady-state emission spectra were recorded using a Spex Fluorolog-3 model FL3-211 fluorescence spectrofluorometer equipped with a R2658P photomultiplier tube (PMT) detector. Unless specified otherwise, the emission spectra were corrected for PMT response. Luminescence quantum yields were measured by the optical dilute method described by Demas and Crosby[29a] using [Ru(bpy)$_3$]Cl$_2$ in acetonitrile (Φ = 0.062 with an excitation wavelength at 436 nm)[29b,c] as the reference and corrected for the refractive index of the solution.[29a] Emission lifetime measurements were performed by a conventional nanosecond pulsed-laser system, which consists of an excitation source with 355 nm output (third harmonic) of a Spectra-Physics Quanta-Ray Q-switched GCR-150-10 pulsed Nd:YAG laser. The solution samples were rigorously degassed with at least four successive freeze−pump−thaw cycles on a high-vacuum line, and the luminescence decay signals were detected by a Hamamatsu R928 PMT and recorded on a Tektronix model TDS-620A (500 MHz, 2 GS s^{-1}) digital oscilloscope. Cyclic voltammetric measurements were conducted using a CH Instruments, Inc. model CHI 620A electrochemical analyzer. Electrochemical measurements were performed at room temperature in DMF with 0.1 M tetrabutylammonium hexafluorophosphate (^{n}Bu$_4$NPF$_6$) as the supporting electrolyte. The reference, working, and counter electrodes were Ag/AgNO$_3$ (0.1 M in acetonitrile), glassy carbon (CH Instruments, Inc.), and platinum wire, respectively. Before the measurements, the working electrode was polished with 1 μm alumina slurry (Linde), followed by 0.3 μm alumina slurry on a microcloth (Buehler Co.), and then rinsed with ultrapure deionized water and sonicated in ultrapure deionized water for 5 min. The working electrode was further polished and sonicated twice and then rinsed under a stream of ultrapure deionized water. Before the electrochemical measurements, all of the solutions were deaerated with prepurified argon gas. The ferrocenium/ferrocene couple ($FeCp_2^{+/0}$) was used as an internal reference at a concentration of approximately 1 × 10^{-3} M. The redox potential of the complex versus SCE, E_{SCE}, was determined by the following equation:[30]

$$E_{SCE} = E + 0.45\ \text{V} - E_{1/2}(FeCp_2^{+/0})_{exp} \quad (1)$$

where E is the observed redox potential of the complex in DMF with 0.1 M ^{n}Bu$_4$NPF$_6$ and $E_{1/2}(FeCp_2^{+/0})_{exp}$ is the observed redox potential of the ferrocenium/ferrocene couple.

Synthesis. *Synthesis of a Functionalized Ligand. 1-Ethynyl-3,5-dibromomethylbenzene.* This was synthesized by modification of literature reported procedures.[25] To a well-stirred degassed solution of 1-ethynyl-3,5-benzenedimethanol[25] (824 mg, 5.09 mmol) in anhydrous THF (20 mL) at −20 °C was added dropwise a degassed solution of PBr_3 (487 mg, 10.17 mmol) in THF (20 mL) under Schlenk conditions using a cannula. After complete addition of the PBr_3 solution, the reaction mixture was allowed to gradually rise to room temperature and stirred overnight. The reaction mixture was then quenched by ice water, and any volatile organic solvent was evaporated under reduced pressure. The remaining aqueous layer was extracted with ethyl acetate twice. The combined organic layers were washed with a saturated NaCl solution, dried over anhydrous $MgSO_4$, and then evaporated under reduced pressure. The crude product was then purified by column chromatography on silica gel, using hexane−ethyl acetate (20:1, v/v) as the eluent. The product was obtained as a white needlelike solid (1.06 g, 3.51 mmol, 69%). ^{1}H NMR (400 MHz, CD_3OD): δ 7.60 (s, 1H, phenyl *H*), 7.55 (s, 2H, phenyl *H*), 4.66 (s, 4H, −C*H*$_2$Br), 3.76 (s, 1 H, −C≡C*H*). Positive EI-MS: *m*/*z* 288 ([M]$^+$).

[3,5-(Me$_3$NCH$_2$)$_2$C$_6$H$_3$C≡CH](OTf)$_2$. This was synthesized by modification of literature reported procedures.[10b] 1-Ethynyl-3,5-dibromomethylbenzene (688 mg, 2.27 mmol) was dissolved in absolute ethanol (20 mL). With stirring, a trimethylamine solution (33% in ethanol, v/v; 2 mL) was added dropwise to the solution mixture. After reaction for 1 h, diethyl ether (100 mL) was added to the solution, and the precipitated white solid was filtered out, washed thoroughly with diethyl ether, and then dried under vacuum to give the bromide salt of the product (859 mg, 2.04 mmol, 90%). ^{1}H NMR (300 MHz, [D$_6$]DMSO): δ 7.99 (s, 1H, phenyl *H*), 7.91 (s, 2H, phenyl *H*), 4.69 (s, 4H, −C*H*$_2$N$^+$(CH$_3$)$_3$), 3.84 (s, 1H, −C≡C*H*), 3.20 (s, 18 H, −CH$_2$N$^+$(C*H*$_3$)$_3$). Metathesis reaction of the bromide salt (859 mg, 2.04 mmol) with AgOTf (1.15 g, 4.49 mmol) gave the trifluoromethanesulfonate salt as an off-white solid (912 mg, 1.47 mmol, 72%). ^{1}H NMR (400 MHz, CD_3OD): δ 7.90 (s, 2H, phenyl *H*), 7.82 (s, 1H, phenyl *H*), 4.61 (s, 4H, −C*H*$_2$N$^+$(CH$_3$)$_3$), 3.85 (s, 1H, −C≡C*H*), 3.18 (s, 18H, −C*H*$_2$N$^+$(C*H*$_3$)$_3$. MS (FAB$^+$): *m*/*z* 544 ([M]$^+$).

4′-[4-(N,N-Dimethylamino)methylphenyl]-2,2′:6′,2″-terpyridine. To a stirring solution of 4′-[4-(bromomethyl)phenyl]-2,2′:6′,2″-terpyridine (300 mg, 0.74 mmol) in dichloromethane (30 mL) was added dropwise a dimethylamine solution in methanol (2.0 M, 1.1 mL). After reaction overnight, the organic solvent was removed by evaporation under reduced pressure. The crude product was dissolved in ethyl acetate and washed with water twice. The organic layer was then dried over anhydrous $MgSO_4$ and evaporated under reduced pressure. Further recrystallization from hot absolute ethanol gave the product as an off-white solid (228 mg, 0.62 mmol, 84%). ^{1}H NMR (400 MHz, $CDCl_3$): δ 8.72 (s, 2H, terpyridyl *H*), 8.68 (d, *J* = 4.4 Hz, 2H, terpyridyl *H*), 8.61 (d, *J* = 8.0 Hz, 2H, terpyridyl *H*), 7.84 (d, *J* = 8.0 Hz, 2H, phenyl *H*), 7.78 (m, 2H, terpyridyl *H*), 7.41 (d, *J* = 8.0 Hz, 2H, phenyl *H*), 7.26 (m, 2H, terpyridyl *H*), 3.44 (s, 2H, −C*H*$_2$N(CH$_3$)$_2$), 2.24 (s, 6H, −CH$_2$N(C*H*$_3$)$_2$). MS (FAB$^+$): *m*/*z* 366 ([M]$^+$).

Synthesis of Platinum(II) Terpyridine Complexes. [Pt{tpy-(C$_6$H$_4$CH$_2$NMe$_2$-4)-4′}Cl](OTf). This was synthesized according to modification of a literature procedure for [Pt(tpy)Cl](OTf)[1a,2a,3a] using 4′-[4-(*N*,*N*-dimethylamino)methylphenyl]-2,2′:6′,2″-terpyridine (220 mg, 0.60 mmol) instead of tpy. It was obtained as an orange solid (360 mg, 0.48 mmol, 80%). ^{1}H NMR (400 MHz, CD_3OD, 323 K): δ 8.97 (d, *J* = 5.6 Hz, 2H, terpyridyl *H*), 8.74 (s, 2H, terpyridyl *H*), 8.60 (d, *J* = 8.0 Hz, 2H, terpyridyl *H*), 8.40 (m, 2H, terpyridyl *H*), 8.12 (d, *J* = 8.0 Hz, 2H, terpyridyl *H*), 7.82 (m, 2H, phenyl *H*), 7.68 (d, *J* = 8.0 Hz, 2H, phenyl *H*), 3.87 (s, 2H, −C*H*$_2$N(CH$_3$)$_2$), 2.48 (s, 6H, −CH$_2$N(C*H*$_3$)$_2$). IR (KBr disk, cm^{-1}): 1153 [s, ν(S═O)]. MS (FAB$^+$): *m*/*z* 596.0 ([M − OTf]$^+$). Elem anal. Calcd for C$_{25}$H$_{22}$ClF$_3$N$_4$O$_3$PtS·CH$_2$Cl$_2$·0.5EtOH: C, 36.50; H, 2.95; N, 6.31. Found: C, 36.68; H, 3.07; N, 6.50.

*[Pt(tpy){C≡CC$_6$H$_4$(CH$_2$NMe$_2$)-4}](OTf) (**1**).* This was synthesized by dehydrohalogenation reaction of [Pt(tpy)Cl](OTf)$_2$ (202 mg, 0.33 mmol) and 1-ethynyl-4-(*N*,*N*-dimethylamino)benzene (171 mg, 1.0 mmol) in the presence of CuI (6 mg, 0.03 mmol) as the catalyst in DMF (10 mL) and distilled triethylamine (1 mL) using modification of a literature procedure for [Pt(tpy)(C≡CC$_6$H$_5$)](OTf).[5,16] After reaction overnight, the solvent was distilled out under vacuum. The crude product was dissolved in a methanol−acetonitrile mixture, and

DOI: 10.1021/acs.inorgchem.6b00513
Inorg. Chem. XXXX, XXX, XXX−XXX

any undissolved solid was filtered off. The filtrate was evaporated under reduced pressure. The crude product was washed with chloroform, acetone, and absolute ethanol, and subsequent recrystallization by diffusion of diethyl ether vapor into the methanol–acetonitrile solution of **1** gave the product as a dark-brown solid (182 mg, 0.25 mmol, 75%). ^{1}H NMR (400 MHz, [D$_6$]DMSO, 353 K): δ 9.24 (d, J = 5.6 Hz, 2H, terpyridyl H), 8.66 (m, 5H, terpyridyl H), 8.52 (m, 2H, terpyridyl H), 7.95 (m, 2H, terpyridyl H), 7.66 (d, J = 8.0 Hz, 2H, phenyl H), 7.56 (d, J = 8.0 Hz, 2H, phenyl H), 4.69 (s, 2H, $-CH_2N(CH_3)_2$), 2.92 (s, 6H, $-CH_2N(CH_3)_2$). IR (KBr disk, cm^{-1}): 2123 [w, ν(C≡C)], 1186 [s, ν(S═O)]. MS (FAB$^+$): m/z 586.1 ([M − OTf]$^+$). Elem anal Calcd for $C_{27}H_{23}F_3N_4O_3PtS\cdot CHCl_3$: C, 39.33; H, 2.83; N, 6.55. Found: C, 39.25; H, 3.08; N, 6.68.

[Pt(tpy){C≡CC$_6$H$_3$(CH$_2$NMe$_2$)$_2$-3,5}](OTf) ***(2)***. The procedure was similar to that for complex **1** except that 1-ethynyl-3,5-bis(*N*,*N*-dimethylamino)benzene (230 mg, 1.0 mmol) was used instead of 1-ethynyl-4-(*N*,*N*-dimethylamino)benzene. The product was obtained as a dark-green solid (165 mg, 0.21 mmol, 63%). ^{1}H NMR (400 MHz, [D$_6$]DMSO, 333 K): δ 9.24 (d, J = 5.2 Hz, 2H, terpyridyl H), 8.69 (m, 5H, terpyridyl H), 8.54 (m, 2H, terpyridyl H), 8.00 (m, 2H, terpyridyl H), 7.38 (s, 2H, phenyl H), 7.23 (s, 1H, phenyl H), 3.53 (s, 4H, $-CH_2N(CH_3)_2$), 2.54 (s, 12H, $-CH_2N(CH_3)_2$). IR (KBr disk, cm^{-1}): 2117 [w, ν(C≡C)], 1168 [s, ν(S═O)]. MS (FAB$^+$): m/z 643.2 ([M − OTf]$^+$). Elem anal. Calcd for $C_{30}H_{30}F_3N_5O_3PtS\cdot 2CHCl_3\cdot CH_3CN$: C, 38.07; H, 3.29; N, 7.84. Found: C, 38.26; H, 3.50; N, 7.60.

[Pt{tpy(C$_6$H$_4$CH$_2$NMe$_3$-4)-4′}{C≡CC$_6$H$_4$(COOH)-4}](OTf)$_2$ ***(3)***. The procedure was similar to that for complex **1** except that [Pt{tpy-(C$_6$H$_4$CH$_2$NMe$_3$-4)-4′}Cl](OTf)$_2$ (300 mg, 0.33 mmol) and 4-ethynylbenzoic acid (146 mg, 1 mmol) were used instead of [Pt(tpy)Cl](OTf) and 1-ethynyl-4-(*N*,*N*-dimethylamino)benzene, respectively. The product was obtained as a red solid (150 mg, 0.15 mmol, 45%). ^{1}H NMR (400 MHz, [D$_6$]DMSO, 353 K): δ 9.29 (d, J = 5.3 Hz, 2H, terpyridyl H), 9.04 (s, 2H, terpyridyl H), 8.85 (d, J = 8.4 Hz, 2H, terpyridyl H), 8.59 (m, 2H, terpyridyl H), 8.32 (d, J = 8.4 Hz, 2H, phenyl H), 8.00 (m, 2H, terpyridyl H), 7.94 (d, J = 8.4 Hz, 2H, phenyl H), 7.86 (d, J = 8.4 Hz, 2H, phenyl H), 7.61 (d, J = 8.4 Hz, 2H, phenyl H), 4.68 (s, 2H, $-CH_2N^+(CH_3)_3$), 3.15 (s, 9H, $-CH_2N^+(CH_3)_3$). IR (KBr disk, cm^{-1}): 2118 [w, ν(C≡C)], 1696 [w, ν(C═O)], 1172 [s, ν(S═O)]. MS (FAB$^+$): m/z 870 ([M − OTf]$^+$). Elem anal. Calcd for $C_{36}H_{30}F_6N_4O_8PtS_2\cdot H_2O$: C, 41.66; H, 3.11; N, 5.40. Found: C, 41.72; H, 3.13; N, 5.39.

[Pt{tpy(C$_6$H$_4$CH$_2$NMe$_3$-4)-4′}{C≡CC$_6$H$_3$(CH$_2$NMe$_2$)$_2$-3,5}](OTf)$_2$ ***(4)***. The procedure was similar to that for complex **3** except that 1-ethynyl-3,5-bis(*N*,*N*-dimethylamino)benzene (230 mg, 1.0 mmol) was used instead of 4-ethynylbenzoic acid. The product was obtained as an orange-red solid (211 mg, 0.2 mmol, 60%). ^{1}H NMR (400 MHz, [D$_6$]DMSO, 353 K): δ 9.26 (d, J = 5.2 Hz, 2H, terpyridyl H), 9.06 (s, 2H, terpyridyl H), 8.87 (d, J = 8.0 Hz, 2H, terpyridyl H), 8.57 (m, 2H, terpyridyl H), 8.33 (d, J = 8.0 Hz, 2H, phenyl H), 8.00 (m, 2H, terpyridyl H), 7.87 (d, J = 8.0 Hz, 2H, phenyl H), 7.56 (s, 2H, phenyl H), 7.37 (s, 1H, phenyl H), 4.69 (s, 2H, $-CH_2N^+(CH_3)_3$), 3.89 (s, 4H, $-CH_2N(CH_3)_2$), 3.15 (s, 9H, $-CH_2N^+(CH_3)_3$), 2.53 (s, 12H, $-CH_2N(CH_3)_2$). IR (KBr disk, cm^{-1}): 2117 [w, ν(C≡C)], 1184 [s, ν(S═O)]. MS (FAB$^+$): m/z 940.2 ([M − OTf]$^+$). Elem anal Calcd for $C_{41}H_{44}F_6N_6O_6PtS_2\cdot 2CHCl_3$: C, 38.87; H, 3.49; N, 6.32. Found: C, 38.54; H, 3.69; N, 6.04.

[Pt{tpy(C$_6$H$_4$CH$_2$NMe$_3$-4)-4′}{C≡CC$_6$H$_4$(CH$_2$NMe$_2$)-4}](OTf)$_2$ ***(5)***. The procedure was similar to that for complex **3** except that 1-ethynyl-4-(*N*,*N*-dimethylamino)benzene (171 mg, 1.0 mmol) was used instead of 4-ethynylbenzoic acid. The product was obtained as a green solid (255 mg, 0.25 mmol, 75%). ^{1}H NMR (400 MHz, [D$_6$]DMSO, 333 K): δ 9.27 (d, J = 6.8 Hz, 2H, terpyridyl H), 9.08 (s, 2H, terpyridyl H), 8.88 (d, J = 8.0 Hz, 2H, terpyridyl H), 8.58 (m, 2H, terpyridyl H), 8.34 (d, J = 8.0 Hz, 2H, phenyl H), 7.99 (m, 2H, terpyridyl H), 7.86 (d, J = 8.0 Hz, 2H, phenyl H), 7.60 (d, J = 8.0 Hz, 2H, phenyl H), 7.47 (d, J = 8.0 Hz, 2H, phenyl H), 4.67 (s, 2H, $-CH_2N^+(CH_3)_3$), 4.18 (s, 2H, $-CH_2N(CH_3)_2$), 3.15 (s, 9H, $-CH_2N^+(CH_3)_3$), 2.70 (s, 6H, $-CH_2N(CH_3)_2$). IR (KBr disk, cm^{-1}) 2119 [w, ν(C≡C)], 1169 [s, ν(S═O)]. MS (FAB$^+$): m/z 883.1 ([M − OTf]$^+$). Elem anal. Calcd for $C_{38}H_{37}F_6N_5O_6PtS_2\cdot 2H_2O$: C, 42.70; H, 3.87; N, 6.55. Found: C, 42.59; H, 3.95; N, 6.66.

[Pt{tpy(C$_6$H$_4$CH$_2$NMe$_3$-4)-4′}{C≡CC$_6$H$_4$(CH$_2$NH$_2$)-4}](OTf)$_2$ ***(6)***. The procedure was similar to that for complex **3** except that 4-ethynylbenzylamine (145 mg, 1.0 mmol) was used instead of 4-ethynylbenzoic acid. The product was obtained as a dark-brown solid (203 mg, 0.20 mmol, 61%). ^{1}H NMR (400 MHz, [D$_6$]DMSO, 353 K): δ 9.28 (d, J = 4.8 Hz, 2H, terpyridyl H), 9.07 (s, 2H, terpyridyl H), 8.88 (m, 2H, terpyridyl H), 8.57 (m, 2H, terpyridyl H), 8.34 (d, J = 8.0 Hz, 2H, phenyl H), 8.00 (m, 2H, terpyridyl H), 7.87 (d, J = 8.0 Hz, 2H, phenyl H), 7.57 (d, J = 8.0 Hz, 2H, phenyl H), 7.45 (d, J = 8.0 Hz, 2H, phenyl H), 4.69 (s, 2H, $-CH_2N^+(CH_3)_3$), 4.06 (s, 2H, $-CH_2NH_2$), 3.13 (s, 9H, $-CH_2N^+(CH_3)_3$). IR (KBr disk, cm^{-1}): 2118 [w, ν(C≡C)], 1169 [s, ν(S═O)]. MS (FAB$^+$): m/z 855.2 ([M − OTf]$^+$). Elem anal. Calcd for $C_{36}H_{33}F_6N_5O_6PtS_2\cdot CH_2Cl_2\cdot 0.5CH_3CN$: C, 40.11; H, 3.28; N, 6.68. Found: C, 40.30; H, 3.30; N, 6.68.

[Pt{tpy(C$_6$H$_4$CH$_2$NMe$_2$-4)-4′}{C≡CC$_6$H$_4$(COOH)-4}](OTf) ***(7)***. The procedure was similar to that for complex **3** except that [Pt{tpy-(C$_6$H$_4$CH$_2$NMe$_2$-4)-4′}Cl](OTf) (224 mg, 0.33 mmol) was used instead of [Pt{tpy(C$_6$H$_4$CH$_2$NMe$_3$-4)-4′}Cl](OTf)$_2$. The product was obtained as a brown solid (195 mg, 0.22 mmol, 67%). ^{1}H NMR (400 MHz, [D$_6$]DMSO, 353 K): δ 9.24 (d, J = 5.6 Hz, 2H, terpyridyl H), 9.01 (s, 2H, terpyridyl H), 8.85 (d, J = 8.0 Hz, 2H, terpyridyl H), 8.54 (m, 2H, terpyridyl H), 8.21 (d, J = 8.0 Hz, 2H, phenyl H), 7.97 (m, 2H, terpyridyl H), 7.93 (d, J = 8.0 Hz, 2H, phenyl H), 7.73 (d, J = 8.0 Hz, 2H, phenyl H), 7.60 (d, J = 8.0 Hz, 2H, phenyl H), 4.06 (s, 2H, $-CH_2N(CH_3)_2$), 2.58 (s, 6H, $-CH_2N(CH_3)_2$). IR (KBr disk, cm^{-1}): 2117 [w, ν(C≡C)], 1186 [s, ν(S═O)]. MS (FAB$^+$): m/z 706.1 ([M − OTf]$^+$). Elem anal. Calcd for $C_{34}H_{27}F_3N_4O_5PtS\cdot 1.5CHCl_3\cdot 0.5CH_3CN$: C, 41.54; H, 2.87; N, 5.97. Found: C, 41.69; H, 3.07; N, 5.65.

[Pt{tpy(C$_6$H$_4$CH$_2$NMe$_2$-4)-4′}{C≡CC$_6$H$_4$–(COOCH$_3$)-4}](OTf) ***(8)***. The procedure was similar to that for complex **7** except that methyl 4-ethynylbenzoate (106 mg, 1.0 mmol) was used instead of 4-ethynylbenzoic acid. The product was obtained as a dark-brown solid (198 mg, 0.23 mmol, 69%). ^{1}H NMR (300 MHz, CD$_3$CN, 298 K): δ 8.46 (d, J = 5.2 Hz, 2H, terpyridyl H), 8.14 (m, 6H, terpyridyl H), 7.60–7.73 (m, 6H, phenyl and terpyridyl H), 7.40 (d, J = 6.0 Hz, 2H, phenyl H), 7.14 (d, J = 6.0 Hz, 2H, phenyl H), 4.14 (s, 2H, $-CH_2N(CH_3)_2$), 3.89 (s, 3H, $-COOCH_3$), 2.71 (s, 6H, $-CH_2N(CH_3)_2$). IR (KBr disk, cm^{-1}): 2118 [w, ν(C≡C)], 1195 [s, ν(S═O)]. MS (FAB$^+$): m/z 720.2 ([M − OTf]$^+$). Elem anal. Calcd for $C_{35}H_{29}F_3N_4O_5PtS\cdot 1.5CHCl_3$: C, 41.80; H, 2.93; N, 5.34. Found: C, 41.60; H, 3.25; N, 5.36.

[Pt{tpy(C$_6$H$_4$CH$_2$NMe$_2$-4)-4′}(C≡CC$_6$H$_5$)](OTf) ***(9)***. The procedure was similar to that for complex **7** except that 4-phenylacetylene (102 mg, 1.0 mmol) was used instead of 4-ethynylbenzoic acid. The product was obtained as a purple-brown solid (155 mg, 0.19 mmol, 58%). ^{1}H NMR (400 MHz, [D$_6$]DMSO, 353 K): δ 9.21 (d, J = 4.8 Hz, 2H, terpyridyl H), 8.95 (s, 2H, terpyridyl H), 8.83 (d, J = 8.0 Hz, 2H, terpyridyl H), 8.52 (m, 2H, terpyridyl H), 8.20 (d, J = 8.0 Hz, 2H, phenyl H), 7.95 (m, 2H, terpyridyl H), 7.70 (d, J = 8.0 Hz, 2H, phenyl H), 7.50 (d, J = 8.0 Hz, 2H, phenyl H), 7.34 (d, J = 8.0 Hz, 2H, phenyl H), 7.27 (m, 1H, phenyl H), 4.01 (s, 2H, $-CH_2N(CH_3)_2$), 2.56 (s, 6H, $-CH_2N(CH_3)_2$). IR (KBr disk, cm^{-1}): 2118 [w, ν(C≡C)], 1166 [s, ν(S═O)]. MS (FAB$^+$): m/z 662.2 ([M − OTf]$^+$). Elem anal. Calcd for $C_{34}H_{29}F_3N_4O_5PtS\cdot 2.5CHCl_3\cdot 0.5CH_3CN$: C, 38.77; H, 2.76; N, 5.57. Found: C, 38.85; H, 3.02; N, 5.59.

[Pt{tpy(C$_6$H$_4$CH$_2$NMe$_2$-4)-4′}{C≡CC$_6$H$_4$(CH$_2$NMe$_3$)-4}](OTf)$_2$ ***(10)***. The procedure was similar to that for complex **7** except that [HC≡CC$_6$H$_4$CH$_2$NMe$_3$-4](OTf) (337 mg, 1.0 mmol) was used instead of 4-ethynylbenzoic acid. The product was obtained as a dark-brown solid (239 mg, 0.23 mmol, 70%). ^{1}H NMR (400 MHz, CD$_3$CN, 323 K): δ 9.19 (d, J = 4.8 Hz, 2H, terpyridyl H), 8.56 (s, 2H, terpyridyl H), 8.43 (m, 4H, terpyridyl H), 8.06 (d, J = 8.0 Hz, 2H, phenyl H), 7.89 (d, J = 8.0 Hz, 2H, phenyl H), 7.80 (m, 2H, terpyridyl H), 7.62 (d, J = 8.0 Hz, 2H, phenyl H), 7.47 (d, J = 8.0 Hz, 2H, phenyl H), 4.45 (s, 2H, $-CH_2N^+(CH_3)_3$), 4.31 (s, 2H, $-CH_2N(CH_3)_2$), 3.06 (s, 9H, $-CH_2N^+(CH_3)_3$), 2.79 (s, 6H, $-CH_2N(CH_3)_2$). IR (KBr disk,

DOI: 10.1021/acs.inorgchem.6b00513
Inorg. Chem. XXXX, XXX, XXX–XXX

cm^{-1}): 2125 [w, ν(C≡C)], 1165 [s, ν(S═O)]. MS (FAB^+): m/z 883.3 ([M − OTf]$^+$). Elem anal. Calcd for $C_{38}H_{37}F_6N_5O_6PtS_2$·1.5$CHCl_3$: C, 39.14; H, 3.20; N, 5.78. Found: C, 38.97; H, 3.50; N, 5.93.

[Pt(tBu$_3$tpy){C≡CC$_6$H$_4$(CH$_2$NMe$_2$)-4}](OTf) ***(11)***. The procedure was similar to that for complex **5** except that [Pt(*t*Bu$_3$tpy)Cl](OTf) (258 mg, 0.33 mmol) was used instead of [Pt{tpy(C$_6$H$_4$CH$_2$NMe$_2$-4)-4′}Cl](OTf). The product was obtained as an orange solid (182 mg, 0.20 mmol, 61%). ^{1}H NMR (400 MHz, [D$_6$]DMSO, 353 K): δ 9.10 (d, J = 6.0 Hz, 2H, terpyridyl *H*), 8.71 (s, 2H, terpyridyl *H*), 8.67 (m, 2H, terpyridyl *H*), 7.91 (m, 2H, terpyridyl *H*), 7.57 (d, J = 8.0 Hz, 2H, phenyl *H*), 7.49 (d, J = 8.0 Hz, 2H, phenyl *H*), 4.23 (s, 2H, −C*H*$_2$N(CH$_3$)$_2$), 2.74 (s, 6H, −CH$_2$N(C*H*$_3$)$_2$), 1.57 (s, 9H, −C(C*H*$_3$)$_3$), 1.48 (s, 18H, −C(C*H*$_3$)$_3$). IR (KBr disk, cm^{-1}): 2103 [w, ν(C≡C)], 1165 [s, ν(S═O)]. MS (FAB^+): m/z 754 ([M − OTf]$^+$). Elem anal. Calcd for $C_{39}H_{47}F_3N_4O_3PtS$·2$CHCl_3$·0.5CH_3CN: C, 46.10; H, 4.84; N, 5.76. Found: C, 46.10; H, 4.74; N, 5.64.

[Pt(tBu$_3$tpy){C≡CC$_6$H$_3$(CH$_2$NMe$_2$)$_2$-3,5}](OTf) ***(12)***. The procedure was similar to that for complex **4** except that [Pt(*t*Bu$_3$tpy)Cl](OTf) (258 mg, 0.33 mmol) was used instead of [Pt{tpy(C$_6$H$_4$CH$_2$NMe$_3$-4)-4′}Cl](OTf)$_2$. The product was obtained as an orange solid (203 mg, 0.21 mmol, 64%). ^{1}H NMR (400 MHz, [D$_6$]DMSO, 353 K): δ 9.08 (d, J = 6.4 Hz, 2H, terpyridyl *H*), 8.72 (s, 2H, terpyridyl *H*), 8.68 (m, 2H, terpyridyl *H*), 7.91 (m, 2H, terpyridyl *H*), 7.61 (s, 2H, phenyl *H*), 7.41 (s, 1H, phenyl *H*), 4.06 (s, 4H, −C*H*$_2$N(CH$_3$)$_2$), 2.64 (s, 12H, −CH$_2$N(C*H*$_3$)$_2$), 1.57 (s, 9H, −C(C*H*$_3$)$_3$), 1.48 (s, 18H, −C(C*H*$_3$)$_3$). IR (KBr disk, cm^{-1}): 2117 [w, ν(C≡C)], 1165 [s, ν(S═O)]. MS (FAB^+): m/z 811 ([M − OTf]$^+$). Elem anal. Calcd for $C_{42}H_{54}F_3N_5O_3PtS$·2.5$CHCl_3$·0.5CH_3CN: C, 42.69, ;H, 4.57; N, 6.02. Found: C, 42.41; H, 4.51; N, 6.33.

[Pt(tBu$_3$tpy){C≡CC$_6$H$_3$(OH)$_2$-3,5}](OTf) ***(13)***. The procedure was similar to that for complex **11** except that 1-ethynyl-3,5-dihydroxybenzene (134 mg, 1.0 mmol) was used instead of 1-ethynyl-4-(*N*,*N*-dimethylamino)benzene. The product was obtained as an orange solid (186 mg, 0.21 mmol, 64%). ^{1}H NMR (400 MHz, [D$_6$]DMSO, 353 K): δ 1.47 (s, 18H, −C(C*H*$_3$)$_3$), 1.57 (s, 9H, −C(C*H*$_3$)$_3$), 6.19 (t, J = 2 Hz, 1H, phenyl *H*), 6.36 (t, J = 2 Hz, 2H, phenyl *H*), 7.95 (m, 2H, terpyridyl *H*), 8.65 (br, 2H, −O*H*), 8.69 (s, 2H, terpyridyl *H*), 8.89 (s, 2H, terpyridyl *H*), 9.07 (d, J = 6.0 Hz, 2H, terpyridyl *H*). IR (KBr disk, cm^{-1}): 2140 [w, ν(C≡C)], 1158 [s, ν(S═O)]. Positive FAB-MS: m/z 729.3 ([M − OTf]$^+$). Elem anal. Calcd for $C_{36}H_{40}F_3N_3O_5PtS$·H_2O·0.5CH_3CN: C, 48.44; H, 4.78; N, 5.34. Found: C, 48.17; H, 4.76; N, 5.17.

[Pt{tpy(C$_6$H$_4$CH$_2$NMe$_3$-4)-4′}{C≡CC$_6$H$_4$(OH)-3}](OTf)$_2$ ***(14)***. The procedure was similar to that for complex **3** except that 3-ethynylphenol (132 mg, 1.0 mmol) was used instead of 4-ethynylbenzoic acid. The product was obtained as a brown solid (252 mg, 0.23 mmol, 71%). ^{1}H NMR (400 MHz, [D$_6$]DMSO, 353 K): δ 3.15 (s, 9H, −CH$_2$N$^+$(C*H*$_3$)$_3$), 4.68 (s, 2H, −C*H*$_2$N$^+$(CH$_3$)$_3$), 6.72 (d, J = 8.0 Hz, 1H, phenyl *H*), 6.77 (d, J = 8.0 Hz, 1H, phenyl *H*), 6.95 (m, 1H, phenyl *H*), 7.13 (s, 1H, phenyl *H*), 7.87 (d, J = 8.0 Hz, 2H, phenyl *H*), 8.00 (m, 2H, terpyridyl *H*), 8.33 (d, J = 8.0 Hz, 2H, phenyl *H*), 8.56 (m, 2H, terpyridyl *H*), 8.86 (d, J = 8.0 Hz, 2H, terpyridyl *H*), 9.05 (s, 2H, terpyridyl *H*), 9.10 (s, 1H, −O*H*), 9.28 (d, J = 6.0 Hz, 2H, terpyridyl *H*). IR (KBr disk, cm^{-1}): 2111 [w, ν(C≡C)], 1276 [s, ν(C−O)], 1162 [s, ν(S═O)]. Positive FAB-MS: m/z 842.1 ([M − OTf]$^+$). Elem anal. Calcd for $C_{35}H_{30}F_6N_4O_7PtS_2$·EtOH·$H_2O$: C, 42.09; H, 3.63; N, 5.31. Found: C, 41.97; H, 3.33; N, 5.62.

[Pt(tBu$_3$tpy){C≡CC$_6$H$_4$−(OH)-3](OTf) ***(15)***. The procedure was similar to that for complex **14** except that [Pt(*t*Bu$_3$tpy)Cl](OTf) (258 mg, 0.33 mmol) was used instead of [Pt{tpy(C$_6$H$_4$CH$_2$NMe$_3$-4)-4′}Cl](OTf)$_2$. The product was obtained as an orange solid (185 mg, 0.21 mmol, 64%). ^{1}H NMR (400 MHz, CD_3CN, 298 K): δ 1.44 (s, 18H, −C(C*H*$_3$)$_3$), 1.53 (s, 9H, −C(C*H*$_3$)$_3$), 6.74 (d, J = 8.0 Hz, 1H, phenyl *H*), 6.87 (d, J = 8.0 Hz, 1H, phenyl *H*), 6.99 (s, 1H, phenyl *H*), 7.13 (m, 1H, phenyl *H*), 7.66 (m, 1H, terpyridyl *H*), 7.74 (m, 1H, terpyridyl *H*), 7.85 (br, 1H, −O*H*), 8.26−8.32 (m, 4H, terpyridyl *H*), 8.74 (d, J = 6.0 Hz, 1H, terpyridyl *H*), 8.78 (d, J = 6.0 Hz, 1H, terpyridyl *H*). IR (KBr disk, cm^{-1}): 2117 [w, ν(C≡C)], 1157 [s, ν(S═O)]. Positive FAB-MS: m/z 713.1 ([M − OTf]$^+$). Elem anal Calcd for $C_{36}H_{40}F_3N_3O_4PtS$·CH_2Cl_2·0.5CH_3CN: C, 47.13; H, 4.53; N, 5.06. Found: C, 47.34; H, 4.76; N, 5.19.

[Pt{tpy(C$_6$H$_4$CH$_2$NMe$_3$-4)-4′}{C≡CCH$_2$OC$_6$H$_4$(COOH)-4}](OTf)$_2$ ***(16)***. The procedure was similar to that for complex **3** except that 4-(propargyloxy)benzoic acid (190 mg, 1.0 mmol) was used instead of 4-ethynylbenzoic acid. The product was obtained as an orange-brown solid (207 mg, 0.20 mmol, 60%). ^{1}H NMR (400 MHz, [D$_6$]DMSO, 353 K): δ 3.14 (s, 9H, −CH$_2$N$^+$(C*H*$_3$)$_3$), 4.67 (s, 2H, −C*H*$_2$N$^+$(CH$_3$)$_3$), 5.22 (s, 2 H, −C*H*$_2$OC$_6$H$_4$−), 7.23 (d, J = 8.8 Hz, 2H, phenyl *H*), 7.84 (m, 4 H, phenyl *H*), 7.97 (d, J = 8.8 Hz, 2H, terpyridyl *H*), 8.30 (d, J = 8.8 Hz, 2H, phenyl *H*), 8.53 (m, 2 H, terpyridyl *H*), 8.82 (d, J = 8.8 Hz, 2H, terpyridyl *H*), 9.01 (m, 4H, terpyridyl *H*). IR (KBr disk, cm^{-1}): 2126 [w, ν(C≡C)], 1265 [s, ν(C−O)], 1180 [s, ν(S═O)]. Positive FAB-MS: m/z 900.1 ([M − OTf]$^+$). Elem anal. Calcd for $C_{37}H_{32}F_6N_4O_9PtS_2$·EtOH: C, 42.74; H, 3.49; N, 5.11. Found: C, 42.64; H, 3.23; N, 4.89.

[Pt{tpy(C$_6$H$_4$CH$_2$NMe$_3$-4)-4′}{C≡CCH$_2$OC$_6$H$_4$(OH)-4}](OTf)$_2$ ***(17)***. The procedure was similar to that for complex **3** except that 4-(propargyloxy)phenol (162 mg, 1.0 mmol) was used instead of 4-ethynylbenzoic acid. The product was obtained as a brown solid (240 mg, 0.23 mmol, 71%). ^{1}H NMR (400 MHz, [D$_6$]DMSO, 353 K): δ 3.14 (s, 9H, −CH$_2$N$^+$(C*H*$_3$)$_3$), 4.67 (s, 2H, −C*H*$_2$N$^+$(CH$_3$)$_3$), 5.03 (s, 2H, −C*H*$_2$OC$_6$H$_4$−), 6.77 (d, J = 8.8 Hz, 2H, phenyl *H*), 6.97 (d, J = 8.8 Hz, 2H, phenyl *H*), 7.86 (m, 4H, phenyl and terpyridyl *H*), 8.30 (d, J = 8.8 Hz, 2H, phenyl *H*), 8.54 (m, 2H, terpyridyl *H*), 8.68 (s, 1H, −O*H*), 8.81 (d, J = 8.8 Hz, 2H, terpyridyl *H*), 9.01 (m, 4H, terpyridyl *H*). IR (KBr disk, cm^{-1}): 2111 [w, ν(C≡C)], 1268 [s, ν(C−O)], 1176 [s, ν(S═O)]. Positive FAB-MS: m/z 706.1 ([M − OTf]$^+$). Elem anal. Calcd for $C_{36}H_{32}F_6N_4O_8PtS_2$·$CHCl_3$·EtOH: C, 39.45; H, 3.31; N, 4.72. Found: C, 39.53; H, 3.23; N, 4.74.

[Pt{tpy(C$_6$H$_4$CH$_2$NMe$_2$-4)-4′}{C≡CCH$_2$OC$_6$H$_4$(COOH)-4}](OTf) ***(18)***. The procedure was similar to that for complex **7** except that 4-(propargyloxy)benzoic acid (190 mg, 1.0 mmol) was used instead of 4-ethynylbenzoic acid. The product was obtained as a brown solid (175 mg, 0.20 mmol, 62%). ^{1}H NMR (400 MHz, [D$_6$]DMSO, 353 K): δ 9.00 (m, 4H, terpyridyl *H*), 8.82 (d, J = 8.8 Hz, 2H, terpyridyl *H*), 8.52 (m, 2 H, terpyridyl *H*), 8.24 (d, J = 8.8 Hz, 2H, phenyl *H*), 7.97 (d, J = 8.8 Hz, 2H, terpyridyl *H*), 7.79 (m, 4 H, phenyl *H*), 7.23 (d, J = 8.8 Hz, 2H, phenyl *H*), 5.21 (s, 2H, −C*H*$_2$OC$_6$H$_4$−), 4.27 (s, 2H, −C*H*$_2$N(CH$_3$)$_2$), 2.72 (s, 6H, −CH$_2$N(C*H*$_3$)$_2$). IR (KBr disk, cm^{-1}): 2126 [w, ν(C≡C)], 1276 [s, ν(C−O)], 1180 [s, ν(S═O)]. MS (FAB^+): m/z 736 ([M − OTf]$^+$). Elem anal. Calcd for $C_{35}H_{29}F_3N_4O_6PtS$·1.5$CHCl_3$: C, 41.17; H, 2.89; N, 5.26. Found: C, 40.94; H, 3.24; N, 5.28.

[Pt{tpy(C$_6$H$_4$CH$_2$NMe$_2$-4)-4′}{C≡CCH$_2$OC$_6$H$_4$(OH)-4}](OTf) ***(19)***. The procedure was similar to that for complex **7** except that 4-(propargyloxy)phenol (162 mg, 1.0 mmol) was used instead of 4-ethynylbenzoic acid. The product was obtained as a brown solid (190 mg, 0.21 mmol, 65%). ^{1}H NMR (400 MHz, [D$_6$]DMSO, 353 K): δ 8.96 (s, 2H, terpyridyl *H*), 8.86 (d, J = 5.2 Hz, 2H, terpyridyl *H*), 8.78 (d, J = 8.8 Hz, 2H, terpyridyl *H*), 8.67 (br, 1H, −O*H*), 8.49 (m, 2H, terpyridyl *H*), 8.25 (d, J = 8.8 Hz, 2H, phenyl *H*), 7.79 (m, 4H, phenyl and terpyridyl *H*), 6.94 (d, J = 8.8 Hz, 2H, phenyl *H*), 6.77 (d, J = 8.8 Hz, 2H, phenyl *H*), 4.97 (s, 2 H, −C*H*$_2$OC$_6$H$_4$−), 4.31 (s, 2H, −C*H*$_2$N(CH$_3$)$_2$), 2.76 (s, 6H, −CH$_2$N(C*H*$_3$)$_2$). IR (KBr disk, cm^{-1}): 2118 [w, ν(C≡C)], 1272 [s, ν(C−O)], 1188 [s, ν(S═O)]. MS (FAB^+): m/z 708.2 ([M − OTf]$^+$). Elem anal. Calcd for $C_{34}H_{29}F_3N_4O_5PtS$·2$CHCl_3$: C, 39.43; H, 2.85; N, 5.11. Found: C, 39.53; H, 3.09; N, 5.28.

Measurements at Different pHs. Electronic absorption and emission spectra of the complexes in the aqueous solution (50 mM NaCl) at different pHs were recorded by the addition of 0.02 M HCl or 0.02 M NaOH to the solution mixture. The pH values were determined by a calibrated pH meter using standard buffer solutions of pH 3, 7, and 10. The ionic strength of the solutions was maintained by the presence of 50 mM NaCl.

Determination of pK_a and pK_a* of the Complexes. With reference to previously reported studies,[7d,15] pK_a and pK_a* of the complexes were determined by the UV−vis absorption and emission spectra of the complexes, respectively, using the following equations:

DOI: 10.1021/acs.inorgchem.6b00513
Inorg. Chem. XXXX, XXX, XXX−XXX

$$\log[(A_{max} - A)/(A - A_{min})] = pH - pK_a \quad (2)$$

$$\log[(I_{max} - I)/(I - I_{min})] = pH - pK_a^* \quad (3)$$

where A_{max} and A_{min} are the maximum and minimum MMLCT absorbances of the complexes, respectively, found in the UV−vis absorption measurements at different pHs, and I_{max} and I_{min} are the maximum and minimum ^{3}MMLCT emission intensities of the complexes, respectively, found in the emission measurements of the complex solutions at different pHs.

On the basis of the fitting of the plot of the MMLCT absorbance against the pH of the complex solutions using eq 2, the pK_a values of the complexes can be determined. Similarly, using eq 3 and the plot of the ^{3}MMLCT emission intensity against the pH of the complex solutions, the pK_a* values of the complexes can be determined.

Effect of Dissolved Oxygen in Aqueous Solutions on the ^{3}MMLCT Emission of the Platinum(II) Complexes. Assuming dynamic quenching of the emission of the platinum(II) complex by oxygen in an aqueous buffer solution, the Stern−Volmer equation is[31]

$$I_0/I = 1 + k_q t_0[O_2] \quad (4)$$

where I_0 and I are the emission intensities of the complex in the absence and presence of oxygen, respectively, k_q is the biomolecular reaction rate constant, and τ_0 is the lifetime of the complex in a deoxygenated solution (Table S2 in the SI). With reference to the solubility of oxygen in water at 25 °C (8.26 mg L^{-1})[32a] and the diffusion-controlled limit for the biomolecular reaction between the metal complexes and oxygen in water (~5 × 10^9 M^{-1} s^{-1}),[32b] any change in the dissolved oxygen concentration by 1 mg L^{-1} at 25 °C would only result in an insignificant change in the emission intensity (smaller than 1.6%).

Protocol for Fixed-Cell Confocal Imaging with Different Intracellular pHs. HeLa cells were grown on a 35 mm tissue culture dish in the growth medium containing DMEM with 10% FBS and 1% penicillin/streptomycin and incubated at 37 °C under a 5% CO_2 atmosphere. After the cells reached ~70% confluence, the culture medium was removed and washed gently with PBS (1 mL × 3), and the cells were treated with precooled methanol at −20 °C for 10 min for fixation.[20] After removal of the methanol solution, the fixed cells were washed gently with PBS (1 mL × 3), followed by incubation with 20 μM of complex **3** in serum- and phenol-red-free DMEM with 0.2% DMSO for 1 h at 37 °C under a 5% CO_2 atmosphere.

After incubation with the complex solution, the medium was removed, washed gently with PBS (1 mL × 3), and replaced by the buffer solution of known pH. The buffer solutions contain 125 mM KCl, 20 mM NaCl, 0.5 mM $CaCl_2$, 0.5 mM $MgCl_2$, and 25 mM MES. The fixed cells were treated with the buffer solution for 10 min at room temperature, and confocal imaging was then performed using a Leica TCS SPE confocal microscope with an excitation wavelength at 488 nm. The emission was measured at 750 ± 50 nm.

Protocol for Confocal Imaging of Lysosomes in Live Cells. HeLa cells were grown on a 35 mm tissue culture dish in the growth medium containing DMEM with 10% FBS and 1% penicillin/streptomycin and incubated at 37 °C under a 5% CO_2 atmosphere. After the cells reached ~70% confluence, the culture medium was removed, washed gently with PBS (1 mL × 3), and replaced by 16 μM of complex **7** in serum- and phenol-red-free DMEM with 0.4% DMSO. After incubation at 37 °C under a 5% CO_2 atmosphere for 1 h, the medium was removed and washed gently with PBS (1 mL × 3), and confocal imaging was then performed using a Leica TCS SPE confocal microscope with an excitation wavelength at 488 nm. The emission was measured at 750 ± 50 nm.

Protocol for Costaining Experiments with LysoSensor Green DND-189. Before the imaging experiments, the culture medium was removed, and the cells were washed gently with PBS (1 mL × 3) and then incubated in 1 μM of DND-189 in serum- and phenol-red-free DMEM with 0.1% DMSO. After incubation at room temperature for 15 min, the medium was removed, the cells were washed gently with PBS (1 mL × 3), and confocal imaging was then performed with λ_{ex} = 488 nm and λ_{em} = 750 ± 50 nm for the NIR emission of complex **7** and λ_{em} = 525 ± 25 nm for the green emission of DND-189. The Pearson's colocalization coefficient of the NIR emission of complex **7** with the green emission of DND-189 was determined from image correlation analysis by WCIF *ImageJ*.

■ ASSOCIATED CONTENT

Supporting Information

The Supporting Information is available free of charge on the ACS Publications website at DOI: 10.1021/acs.inorgchem.6b00513.

Synthetic pathways of functionalized tpy and alkynes, UV−vis absorption, emission and excitation spectra, and cyclic voltammograms of representative complexes, electronic absorption spectra and emission spectra of complex **2** in an aqueous solution (50 mM NaCl) at different pHs, electronic absorption and emission spectra of complex **4** in pH 4 and 10 aqueous solutions (50 mM NaCl) at different temperatures, electronic absorption spectra of complexes **3** and **7** in aqueous solutions (50 mM NaCl) at different pHs, emission spectra of complex **3** in aqueous solution (50 mM NaCl) at different pHs, and emission lifetimes of representative complexes in degassed aqueous solution (50 mM NaCl) (PDF)

■ AUTHOR INFORMATION

Corresponding Author

*E-mail: wwyam@hku.hk.

Notes

The authors declare no competing financial interest.

■ ACKNOWLEDGMENTS

V.W.-W.Y. acknowledges support from the University Grants Committee Areas of Excellence Scheme (AoE/P-03/08) and the General Research Fund (HKU 7051/13P) from the Research Grants Council of Hong Kong Special Administrative Region, China. C.Y.-S.C acknowledges the receipt of a Postgraduate Studentship administered by The University of Hong Kong.

■ REFERENCES

(1) (a) Morgan, G. T.; Burstall, F. H. *J. Chem. Soc.* **1934**, *0*, 965. (b) Osborn, R. S.; Rogers, D. *J. Chem. Soc., Dalton Trans.* **1974**, 1002. (c) Miskowski, V. M.; Houlding, V. H. *Inorg. Chem.* **1991**, *30*, 4446. (d) Houlding, V. H.; Miskowski, V. M. *Coord. Chem. Rev.* **1991**, *111*, 145. (e) Connick, W. B.; Henling, L. M.; Marsh, R. E.; Gray, H. B. *Inorg. Chem.* **1996**, *35*, 6261. (f) Connick, W. B.; Marsh, R. E.; Schaefer, W. P.; Gray, H. B. *Inorg. Chem.* **1997**, *36*, 913. (g) Büchner, R.; Cunningham, C. T.; Field, J. S.; Haines, R. J.; McMillin, D. R.; Summerton, G. C. *J. Chem. Soc., Dalton Trans.* **1999**, 711.

(2) (a) Bailey, J. A.; Hill, M. G.; Marsh, R. E.; Miskowski, V. M.; Schaefer, W. P.; Gray, H. B. *Inorg. Chem.* **1995**, *34*, 4591. (b) Morgan, G. T.; Burstall, F. H. *J. Chem. Soc.* **1934**, *0*, 1498. (c) Howe-Grant, M.; Lippard, S. J.; Chalilpoyil, P; Marzilli, L. G. *Inorg. Synth.* **1980**, *20*, 101. (d) Bailey, J. A.; Miskowski, V. M.; Gray, H. B. *Inorg. Chem.* **1993**, *32*, 369.

(3) (a) Jennette, K. W.; Gill, J. T.; Sadownick, J. A.; Lippard, S. J. *J. Am. Chem. Soc.* **1976**, *98*, 6159. (b) Yip, H. K.; Che, C. M.; Zhou, Z. Y.; Mak, T. C. W. *J. Chem. Soc., Chem. Commun.* **1992**, 1369. (c) Yip, H. K.; Cheng, L. K.; Cheung, K. K.; Che, C. M. *J. Chem. Soc., Dalton Trans.* **1993**, 2933. (d) Hill, M. G.; Bailey, J. A.; Miskowski, V. M.; Gray, H. B. *Inorg. Chem.* **1996**, *35*, 4585. (e) Büchner, R.; Field, J. S.; Haines, R. J.; Cunningham, C. T.; McMillin, D. R. *Inorg. Chem.* **1997**, *36*, 3952. (f) Wadas, T. J.; Wang, Q. M.; Kim, Y. J.; Flaschenreim, C.; Blanton, T. N.; Eisenberg, R. *J. Am. Chem. Soc.* **2004**, *126*, 16841.

DOI: 10.1021/acs.inorgchem.6b00513
Inorg. Chem. XXXX, XXX, XXX−XXX

(g) Chakraborty, S.; Wadas, T. J.; Hester, H.; Flaschenreim, C.; Schmehl, R.; Eisenberg, R. *Inorg. Chem.* **2005**, *44*, 6284.
(4) (a) Camerel, F.; Ziessel, R.; Donnio, B.; Bourgogne, C.; Guillon, D.; Schmutz, M.; Iacovita, C.; Bucher, J. P. *Angew. Chem., Int. Ed.* **2007**, *46*, 2659. (b) Yuen, M. Y.; Roy, V. A. L.; Lu, W.; Kui, S. C. F.; Tong, G. S. M.; So, M. H.; Chui, S. S. Y.; Muccini, M.; Ning, J. Q.; Xu, S. J.; Che, C. M. *Angew. Chem., Int. Ed.* **2008**, *47*, 9895.
(5) Yam, V. W. W.; Tang, R. P. L.; Wong, K. M. C.; Cheung, K. K. *Organometallics* **2001**, *20*, 4476.
(6) Yam, V. W. W.; Wong, K. M. C.; Zhu, N. *J. Am. Chem. Soc.* **2002**, *124*, 6506.
(7) (a) Yam, V. W. W.; Chan, K. H. Y.; Wong, K. M. C.; Chu, B. W. K. *Angew. Chem., Int. Ed.* **2006**, *45*, 6169. (b) Tam, A. Y. Y.; Wong, K. M. C.; Yam, V. W. W. *J. Am. Chem. Soc.* **2009**, *131*, 6253. (c) Chan, K. H. Y.; Chow, H. S.; Wong, K. M. C.; Yeung, M. C. L.; Yam, V. W. W. *Chem. Sci.* **2010**, *1*, 477. (d) Chung, C. Y. S.; Li, S. P. Y.; Louie, M. W.; Lo, K. K. W.; Yam, V. W. W. *Chem. Sci.* **2013**, *4*, 2453. (e) Po, C.; Ke, Z.; Tam, A. Y. Y.; Chow, H. F.; Yam, V. W. W. *Chem. - Eur. J.* **2013**, *19*, 15735.
(8) (a) Leung, S. Y. L.; Tam, A. Y. Y.; Tao, C. H.; Chow, H. S.; Yam, V. W. W. *J. Am. Chem. Soc.* **2012**, *134*, 1047. (b) Leung, S. Y. L.; Lam, W. H.; Yam, V. W. W. *Proc. Natl. Acad. Sci. U. S. A.* **2013**, *110*, 7986. (c) Leung, S. Y. L.; Yam, V. W. W. *Chem. Sci.* **2013**, *4*, 4228.
(9) (a) Yam, V. W. W.; Hu, Y. C.; Chan, K. H. Y.; Chung, C. Y. S. *Chem. Commun.* **2009**, 6216. (b) Hu, Y.; Chan, K. H. Y.; Chung, C. Y. S.; Yam, V. W. W. *Dalton Trans.* **2011**, *40*, 12228. (c) Chung, C. Y. S.; Yam, V. W. W. *Chem. - Eur. J.* **2013**, *19*, 13182.
(10) (a) Yu, C.; Wong, K. M. C.; Chan, K. H. Y.; Yam, V. W. W. *Angew. Chem., Int. Ed.* **2005**, *44*, 791. (b) Yu, C.; Chan, K. H. Y.; Wong, K. M. C.; Yam, V. W. W. *Chem. - Eur. J.* **2008**, *14*, 4577.
(11) (a) Yu, C.; Chan, K. H. Y.; Wong, K. M. C.; Yam, V. W. W. *Proc. Natl. Acad. Sci. U. S. A.* **2006**, *103*, 19652. (b) Yeung, M. C. L.; Wong, K. M. C.; Tsang, Y. K. T.; Yam, V. W. W. *Chem. Commun.* **2010**, *46*, 7709. (c) Chung, C. Y. S.; Chan, K. H. Y.; Yam, V. W. W. *Chem. Commun.* **2011**, *47*, 2000. (d) Yeung, M. C. L.; Yam, V. W. W. *Chem. - Eur. J.* **2011**, *17*, 11987. (e) Yeung, M. C. L.; Yam, V. W. W. *Chem. Sci.* **2013**, *4*, 2928.
(12) (a) Chung, C. Y. S.; Yam, V. W. W. *J. Am. Chem. Soc.* **2011**, *133*, 18775. (b) Chung, C. Y. S.; Yam, V. W. W. *Chem. Sci.* **2013**, *4*, 377.
(13) (a) Baggaley, E.; Weinstein, J. A.; Williams, J. A. G. *Coord. Chem. Rev.* **2012**, *256*, 1762. (b) Septiadi, D.; Aliprandi, A.; Mauro, M.; De Cola, L. *RSC Adv.* **2014**, *4*, 25709. (c) Colombo, A.; Fiorini, F.; Septiadi, D.; Dragonetti, C.; Nisic, F.; Valore, A.; Roberto, D.; Mauro, M.; De Cola, L. *Dalton Trans.* **2015**, *44*, 8478. (d) Mauro, M.; Aliprandi, A.; Septiadi, D.; Kehr, N. S.; De Cola, L. *Chem. Soc. Rev.* **2014**, *43*, 4144.
(14) (a) Soini, E.; Hemmila, I. *Clin. Chem.* **1979**, *25*, 353. (b) Licha, K. *Top. Curr. Chem.* **2002**, *222*, 1. (c) Barone, P. W.; Baik, S.; Heller, D. A.; Strano, M. S. *Nat. Mater.* **2005**, *4*, 86. (d) Bashkatov, A. N.; Genina, E. A.; Kochubey, V. I.; Tuchin, V. V. *J. Phys. D: Appl. Phys.* **2005**, *38*, 2543.
(15) (a) Zen, J. M.; Patonay, G. *Anal. Chem.* **1991**, *63*, 2934. (b) Briggs, M. S.; Burns, D. D.; Cooper, M. E.; Gregory, S. J. *Chem. Commun.* **2000**, 2323. (c) Finikova, O.; Galkin, A.; Rozhkov, V.; Cordero, M.; Hägerhäll, C.; Vinogradov, S. *J. Am. Chem. Soc.* **2003**, *125*, 4882. (d) Zhang, Z.; Achilefu, S. *Chem. Commun.* **2005**, 5887. (e) Hilderbrand, S. A.; Weissleder, R. *Chem. Commun.* **2007**, 2747. (f) Tang, B.; Liu, X.; Xu, K. H.; Huang, H.; Yang, G. W.; An, L. G. *Chem. Commun.* **2007**, 3726. (g) Almutairi, A.; Guillaudeu, S. J.; Berezin, M. Y.; Achilefu, S.; Fréchet, J. M. J. *J. Am. Chem. Soc.* **2008**, *130*, 444. (h) Tang, B.; Yu, F.; Li, P.; Tong, L.; Duan, X.; Xie, T.; Wang, X. *J. Am. Chem. Soc.* **2009**, *131*, 3016. (i) Thyagarajan, S.; Leiding, T.; Årsköld, S. P.; Cheprakov, A. V.; Vinogradov, S. A. *Inorg. Chem.* **2010**, *49*, 9909. (j) Lu, H.; Xu, B.; Dong, Y.; Chen, F.; Li, Y.; Li, Z.; He, J.; Li, H.; Tian, W. *Langmuir* **2010**, *26*, 6838. (k) Song, P.; Chen, X.; Xiang, Y.; Huang, L.; Zhou, Z.; Wei, R.; Tong, A. *J. Mater. Chem.* **2011**, *21*, 13470. (l) Chen, S.; Liu, J.; Liu, Y.; Su, H.; Hong, Y.; Jim, C. K. W.; Kwok, R. T. K.; Zhao, N.; Qin, W.; Lam, J. W. Y.; Wong, K. S.; Tang, B. Z. *Chem. Sci.* **2012**, *3*, 1804.
(16) (a) Sonogashira, K.; Takahashi, S.; Hagihara, N. *Macromolecules* **1977**, *10*, 879. (b) Takahashi, S.; Kariya, M.; Yatake, T.; Sonogashira, K.; Hagihara, N. *Macromolecules* **1978**, *11*, 1063.
(17) Michalec, J. F.; Bejune, S. A.; Cuttell, D. G.; Summerton, G. C.; Gertenbach, J. A.; Field, J. S.; Haines, R. J.; McMillin, D. R. *Inorg. Chem.* **2001**, *40*, 2193.
(18) (a) Nelsen, S. F.; Hintz, P. J. *J. Am. Chem. Soc.* **1972**, *94*, 7114. (b) Kontturi, A. K.; Kontturi, K.; Murtomaki, L.; Schiffrin, D. J. *Acta Chem. Scand.* **1992**, *46*, 47. (c) Chen, J.; Wenger, O. S. *Chem. Sci.* **2015**, *6*, 3582.
(19) (a) Tian, H.; Gan, J.; Chen, K.; He, J.; Song, Q. L.; Hou, X. Y. *J. Mater. Chem.* **2002**, *12*, 1262. (b) Petsalakis, I. D.; Kerkines, I. S. K.; Lathiotakis, N. N.; Theodorakopoulos, G. *Chem. Phys. Lett.* **2009**, *474*, 278. (c) Das, P.; Ghosh, A.; Bhatt, H.; Das, A. *RSC Adv.* **2012**, *2*, 3714.
(20) (a) Epstein, J.; Xiao, H.; Oba, B. K. *Blood* **1989**, *74*, 913. (b) Pollice, A. A.; McCoy, J. P., Jr.; Shackney, S. E.; Smith, C. A.; Agarwal, J.; Burnolt, D. R.; Janocko, L. E.; Hornicek, F. J.; Singh, S. G.; Hartsock, R. J. *Cytometry* **1992**, *13*, 432. (c) Dasari, M.; Lee, S.; Sy, J.; Kim, D.; Lee, S.; Brown, M.; Davis, M.; Murthy, N. *Org. Lett.* **2010**, *12*, 3300. (d) Schnell, U.; Dijk, F.; Sjollema, K. A.; Giepmans, B. N. G. *Nat. Methods* **2012**, *9*, 152.
(21) Serum- and phenol-red-free DMEM was used during the incubation of HeLa cells with complex **3** in order to prevent any interference on the emission of the complex by the serum proteins and phenol red dye.
(22) A fairly good Pearson's colocalization coefficient of 0.8 was found in analysis of the colocalization of the NIR emission of complex **7** at λ_{em} = 750 ± 50 nm with the green emission of DND-189 at λ_{em} = 525 ± 25 nm. This may be due to the different emission spectral changes of complex **7** with the pH (in a two-step manner), from that of DND-189 (with a single pK_a value of 5.2), in vitro. Yet, from the merged image (Figure 7d), the more intense NIR emission of complex **7** showed very good colocalization with the intense green emission of DND-189. This supports the pH-responsive NIR emission of complex **7** in live HeLa cells.
(23) Wang, J.; Hanan, G. S. *Synlett* **2005**, *8*, 1251.
(24) Haider, J. M.; Chavarot, M.; Weidner, S.; Sadler, I.; Williams, R. M.; De Cola, L.; Pikramenou, Z. *Inorg. Chem.* **2001**, *40*, 3912.
(25) (a) Steenwinkel, P.; James, S. L.; Grove, D. M.; Veldman, N.; Spek, A. L.; van Koten, G. *Chem. - Eur. J.* **1996**, *2*, 1440. (b) Lang, H.; Köcher, S.; Back, S.; Rheinwald, G.; van Koten, G. *Organometallics* **2001**, *20*, 1968.
(26) Gottardo, C.; Aguirre, A. *Tetrahedron Lett.* **2002**, *43*, 7091.
(27) Negishi, K.; Mashiko, Y.; Yamashita, E.; Otsuka, A.; Hasegawa, T. *Polymers* **2011**, *3*, 489.
(28) Srinivasan, M.; Sankararaman, S.; Hopf, H.; Dix, I.; Jones, P. G. *J. Org. Chem.* **2001**, *66*, 4299.
(29) (a) Crosby, G. A.; Demas, J. N. *J. Phys. Chem.* **1971**, *75*, 991. (b) Himel, C. M.; Mayer, R. T. *Anal. Chem.* **1970**, *42*, 130. (c) Wallace, L.; Rillema, D. P. *Inorg. Chem.* **1993**, *32*, 3836.
(30) Connelly, N. G.; Geiger, W. E. *Chem. Rev.* **1996**, *96*, 877.
(31) Lakowicz, J. R. *Principles of Fluorescence Spectroscopy*, 2nd ed.; Kluwer Academic/Plenum Publishers: New York, 1999.
(32) (a) Montgomery, H. A. C.; Thom, N. S.; Cockburn, A. *J. Appl. Chem.* **1964**, *14*, 280. (b) Demas, J. N.; Diemente, D.; Harris, E. W. *J. Am. Chem. Soc.* **1973**, *95*, 6864.

DOI: 10.1021/acs.inorgchem.6b00513
Inorg. Chem. XXXX, XXX, XXX−XXX